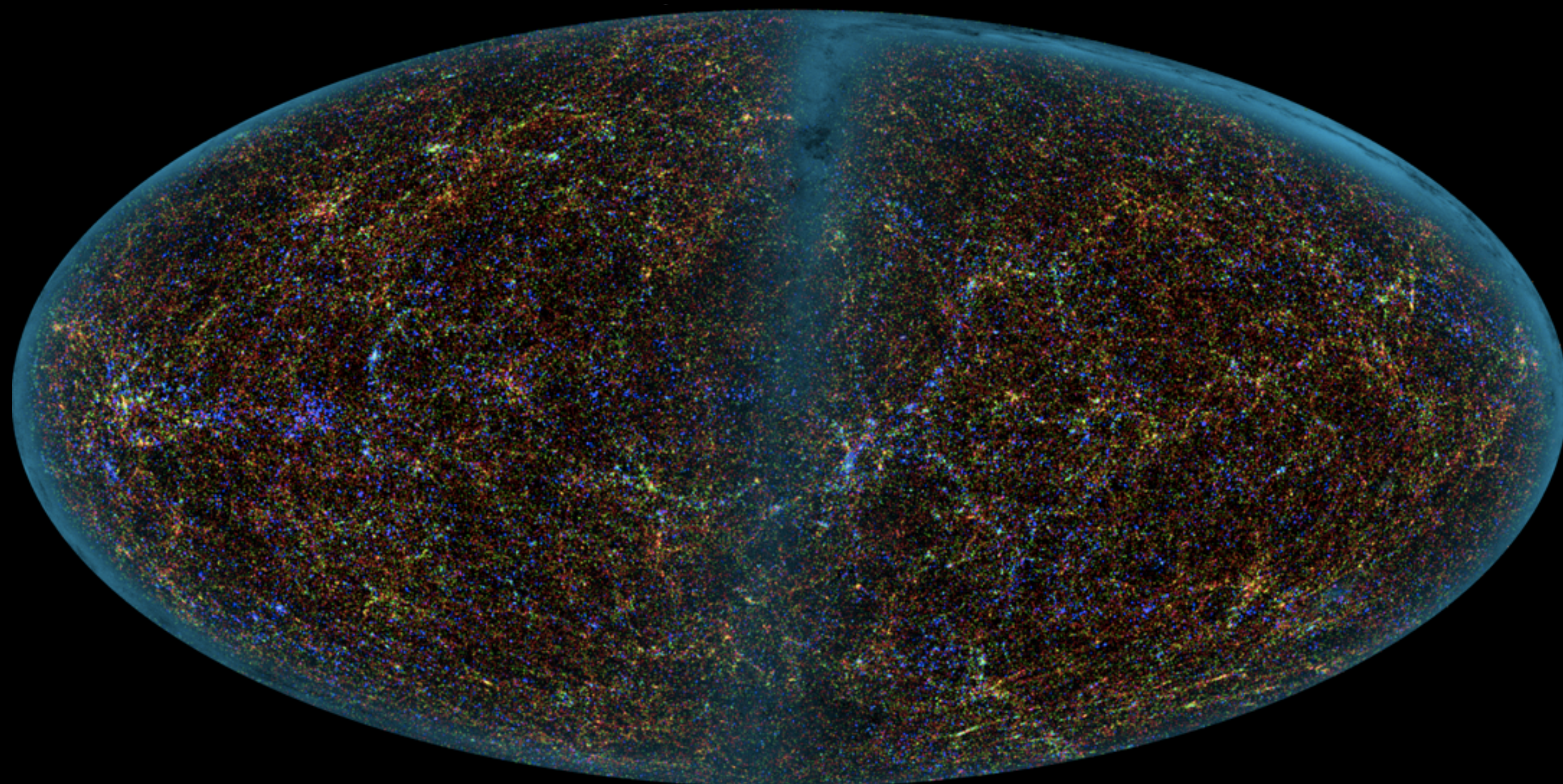


# Cosmology and Large Scale Structure



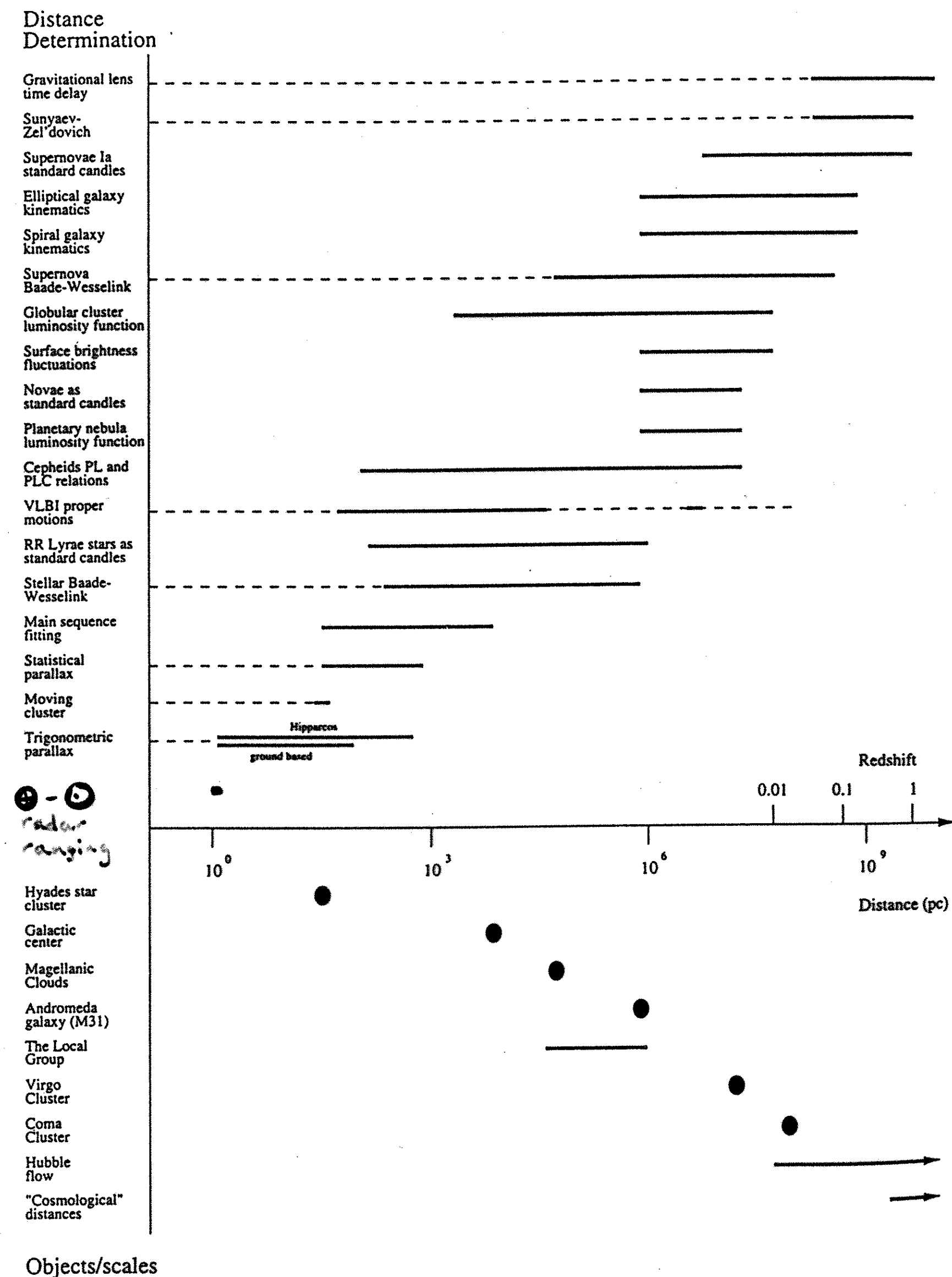
Today  
Distance Scale III  
Tully-Fisher  
Absolute methods  
 $H_0$  tension

*next homework posted*

# Distance Scale Ladder

# Distance Scale

- Solar System
  - earth-sun distance
- Trigonometric Parallax
  - statistical & secular parallax; moving clusters
- Main Sequence Fitting
- Bright Star Standard Candles
  - Cepheids, RR Lyraes, TRGB
- Secondary Distance Indicators
  - Type Ia SN, Tully-Fisher, Fundamental Plane, SB Fluctuations
- Absolute Methods
  - Gravitational lens time delay, SZ effect, water masers



$$\text{distance modulus } m - M = 5 \log(d) - 5$$

# Distance Scale

- Secondary Distance Indicators
  - Tully-Fisher relation
    - luminosity-linewidth relation
  - Baryonic Tully-Fisher relation
    - baryonic mass-flat rotation speed relation

Faber-Jackson relation first noticed as a scaling relation between luminosity and line width in Spiral galaxies. Slope band-dependent.

The line width is a crude estimator of the rotation speed. It provides an estimator of the luminosity which in turn acts as a standard candle to give the distance.

"The result for the Virgo cluster suggests a Hubble constant of 80 km per sec per Mpc"  
- Tully & Fisher (1977)

Tully & Fisher (1977)  
R. B. Tully and J. R. Fisher: Distances to Galaxies

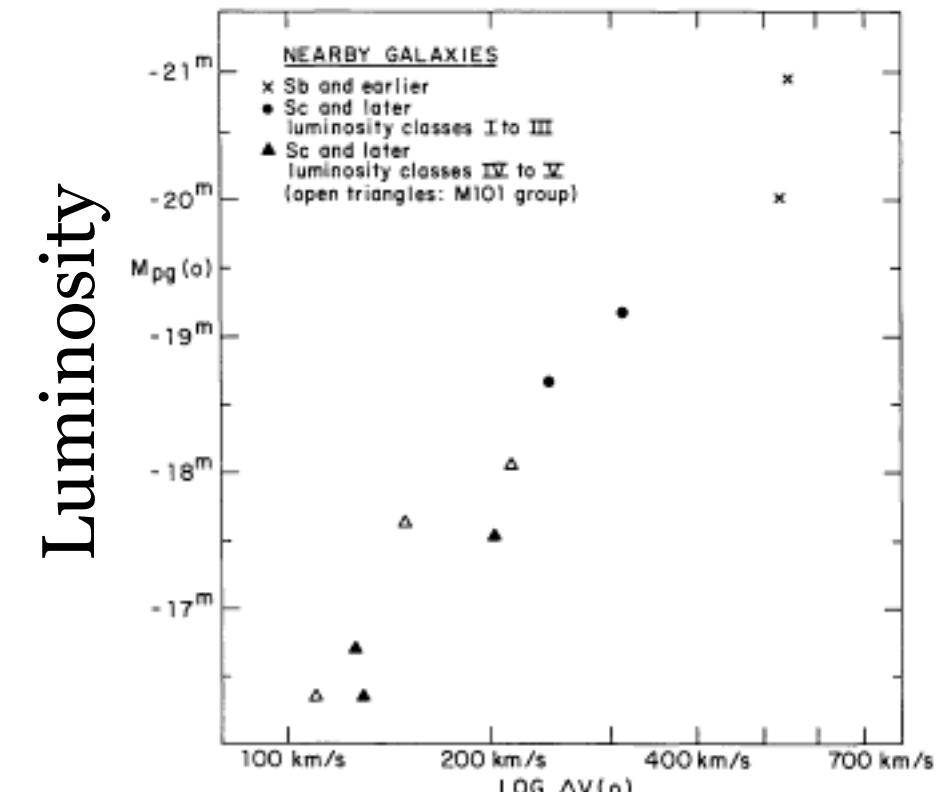
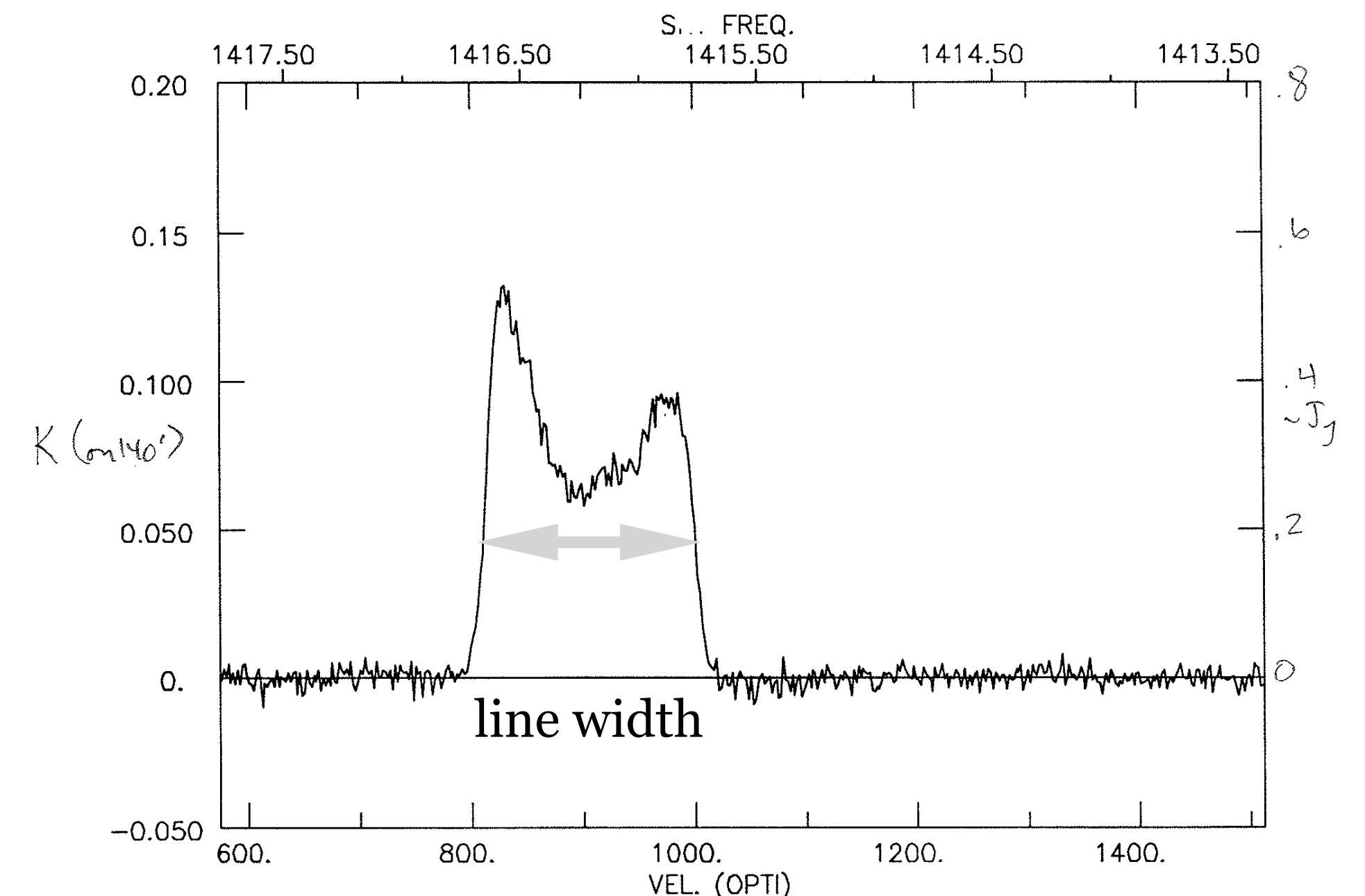


Fig. 1. Absolute magnitude – global profile width relation for nearby galaxies with previously well-determined distances. Crosses are M31 and M81, dots are M33 and NGC 2403, filled triangles are smaller systems in the M81 group and open triangles are smaller systems in the M101 group

line width

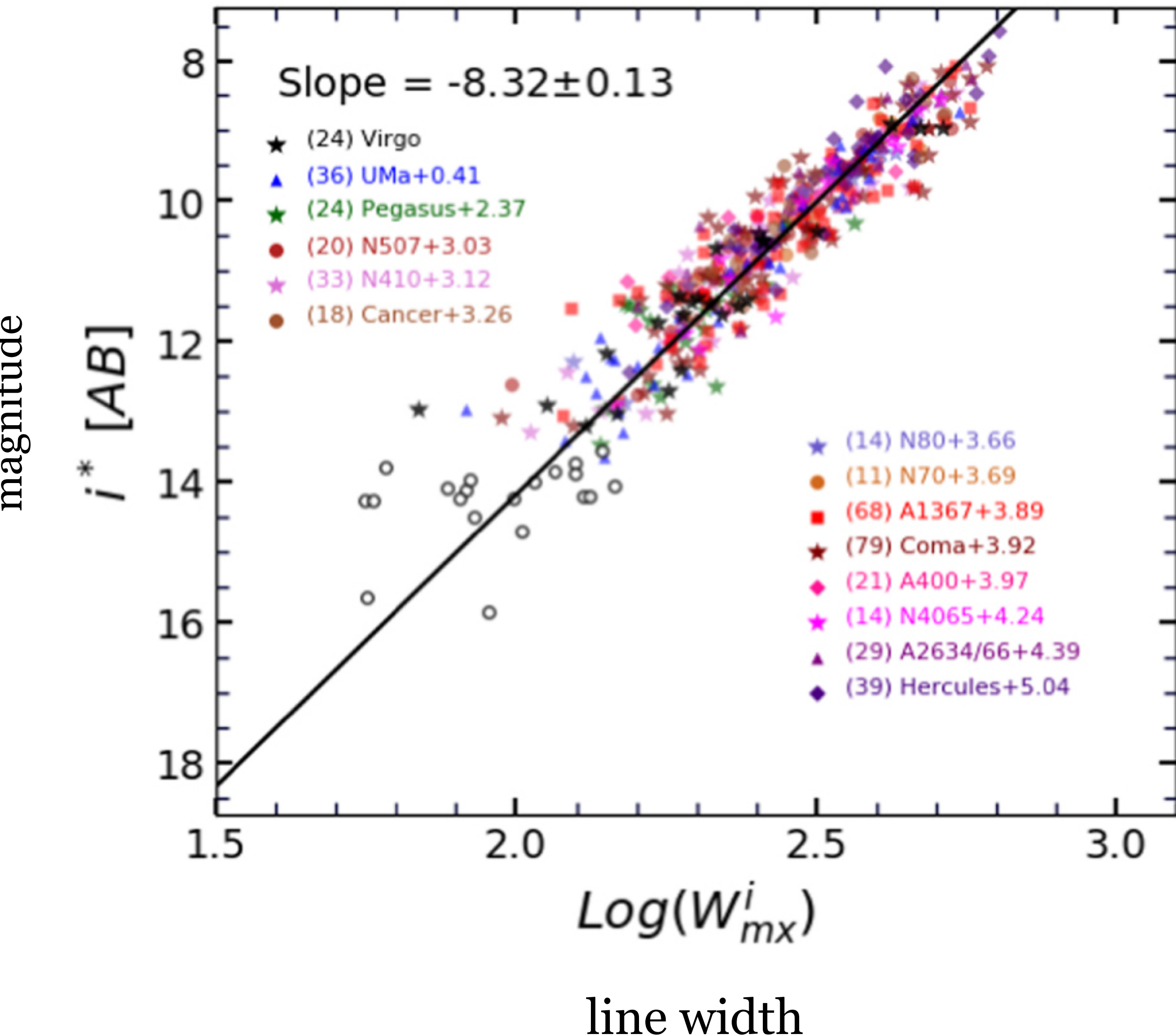


# Tully-Fisher relations

amplitude of line width correlates with luminosity

- Secondary Distance Indicators
  - **Tully-Fisher relation**
    - luminosity-linewidth relation
  - Baryonic Tully-Fisher relation
    - baryonic mass-flat rotation speed relation

Kourkchi, Tully, et al. (2020)



Calibrate TF with galaxies whose distance is known by other means...

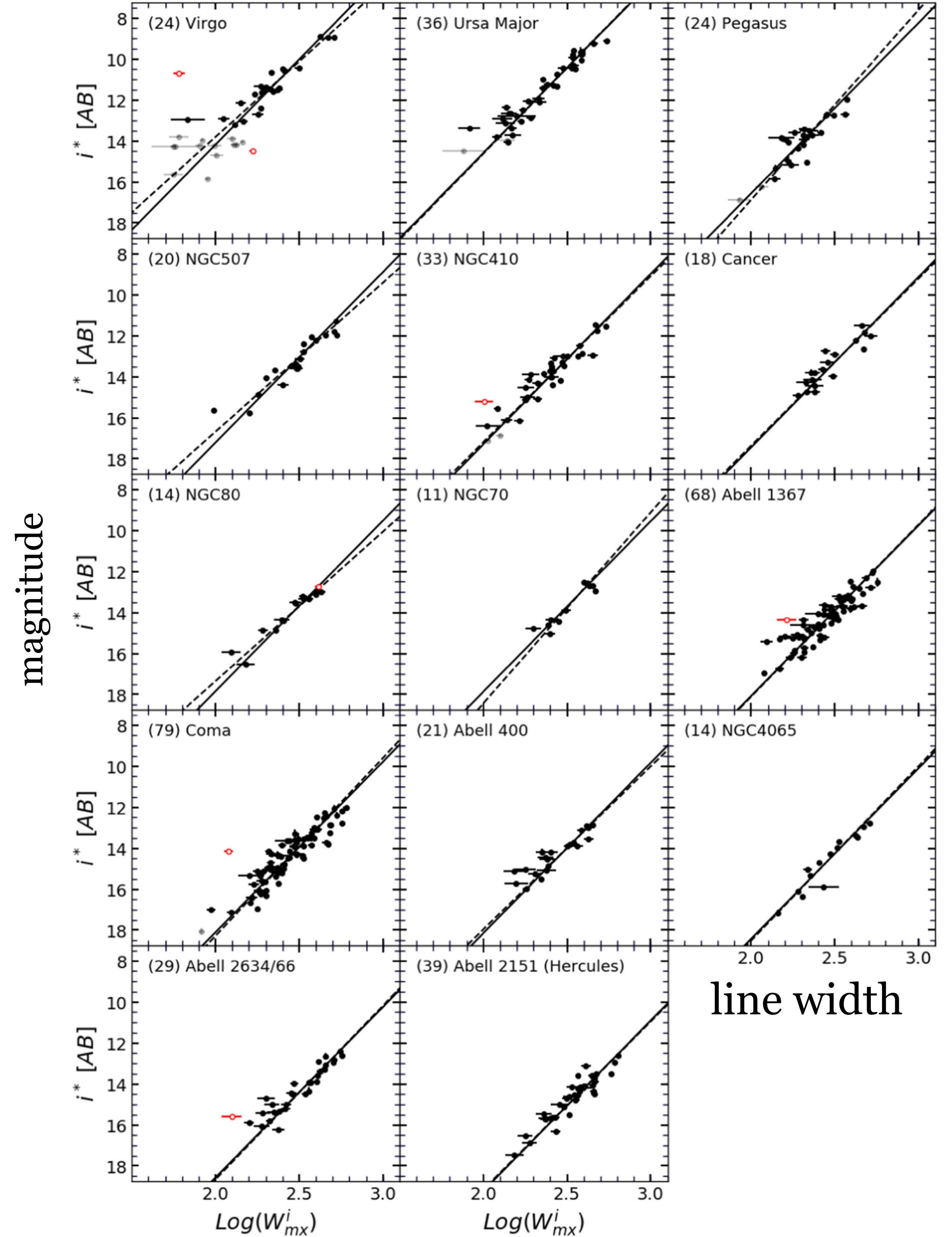
line width

# Tully-Fisher relations

amplitude of line width correlates with luminosity

- Secondary Distance Indicators
  - **Tully-Fisher relation**
    - luminosity-linewidth relation
  - Baryonic Tully-Fisher relation
    - baryonic mass-flat rotation speed relation

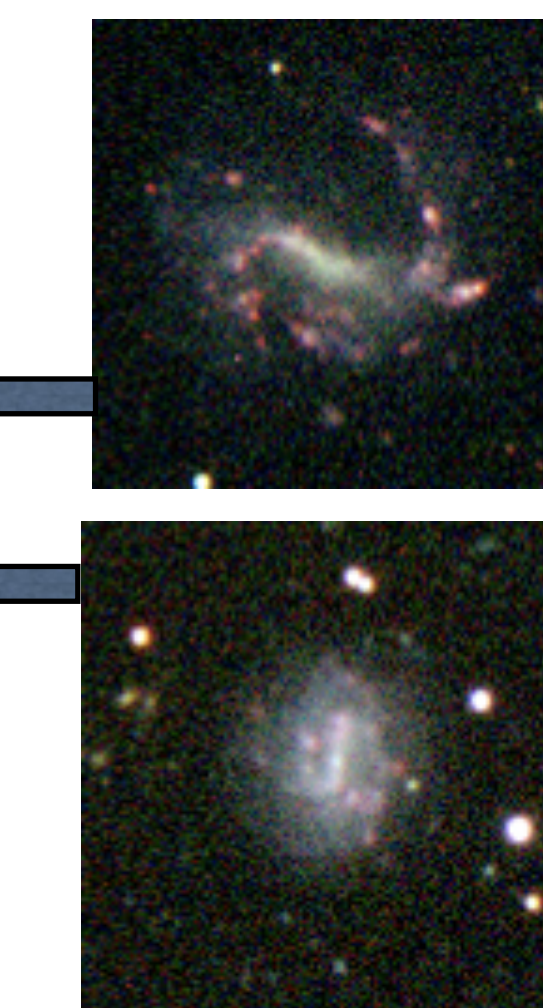
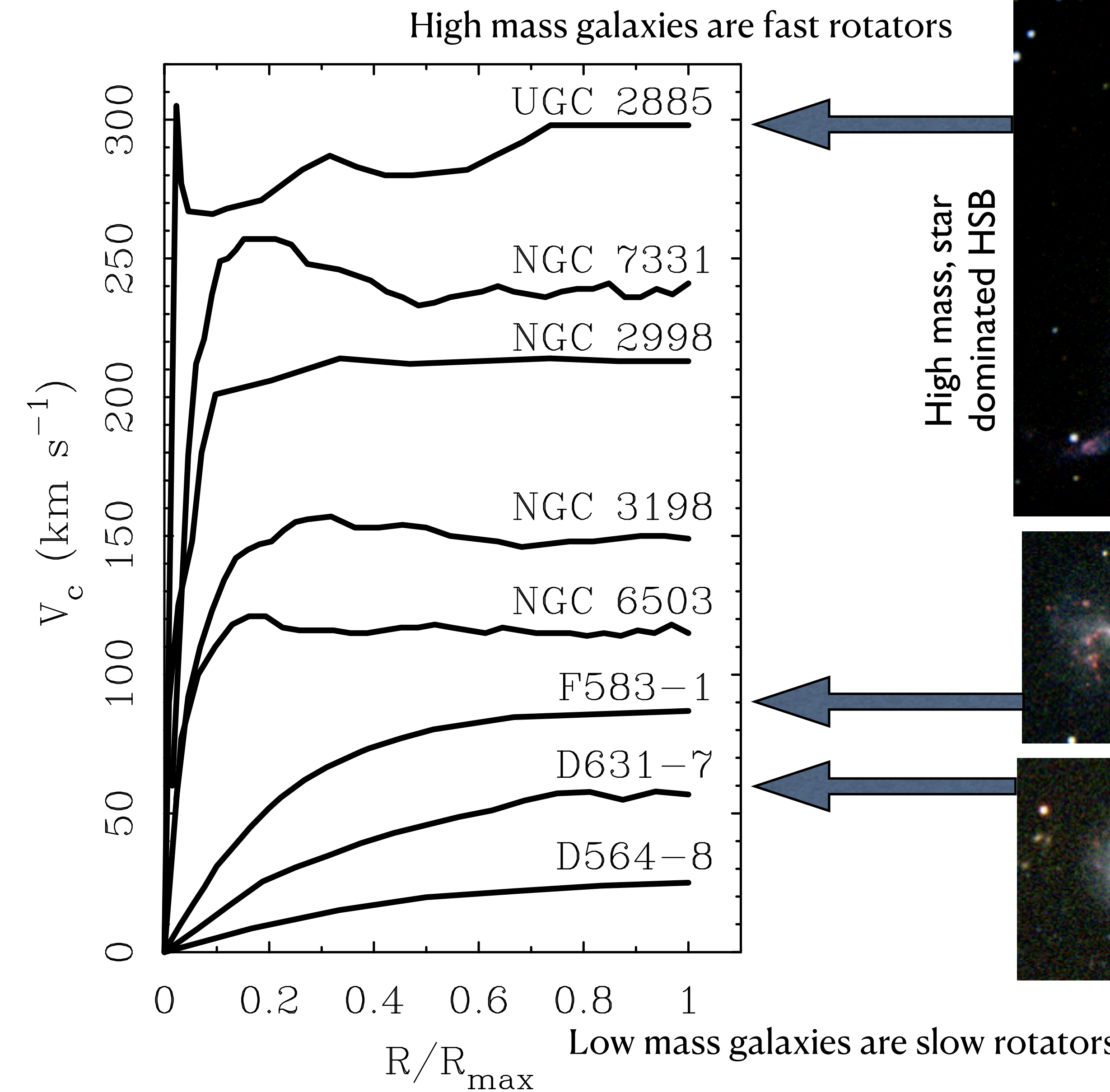
... then apply to more distance galaxies. At right, many clusters are shown.  
One thus gets a distance to every cluster to use to determine  $H_0$ .



# Tully-Fisher relations

amplitude of flat rotation correlates with mass

- Secondary Distance Indicators
  - Tully-Fisher relation
    - luminosity-linewidth relation
  - **Baryonic Tully-Fisher relation**
    - baryonic mass-flat rotation speed relation

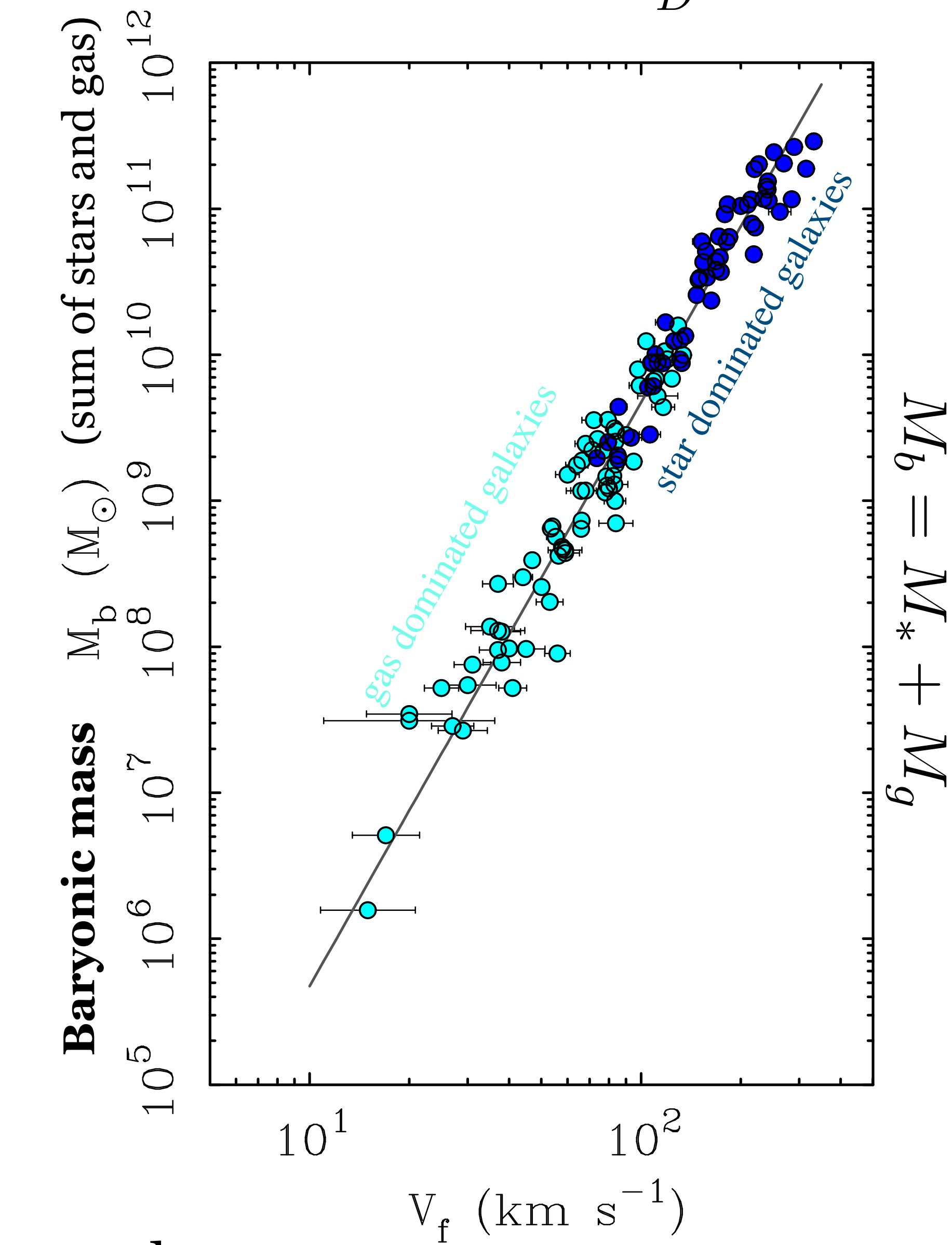
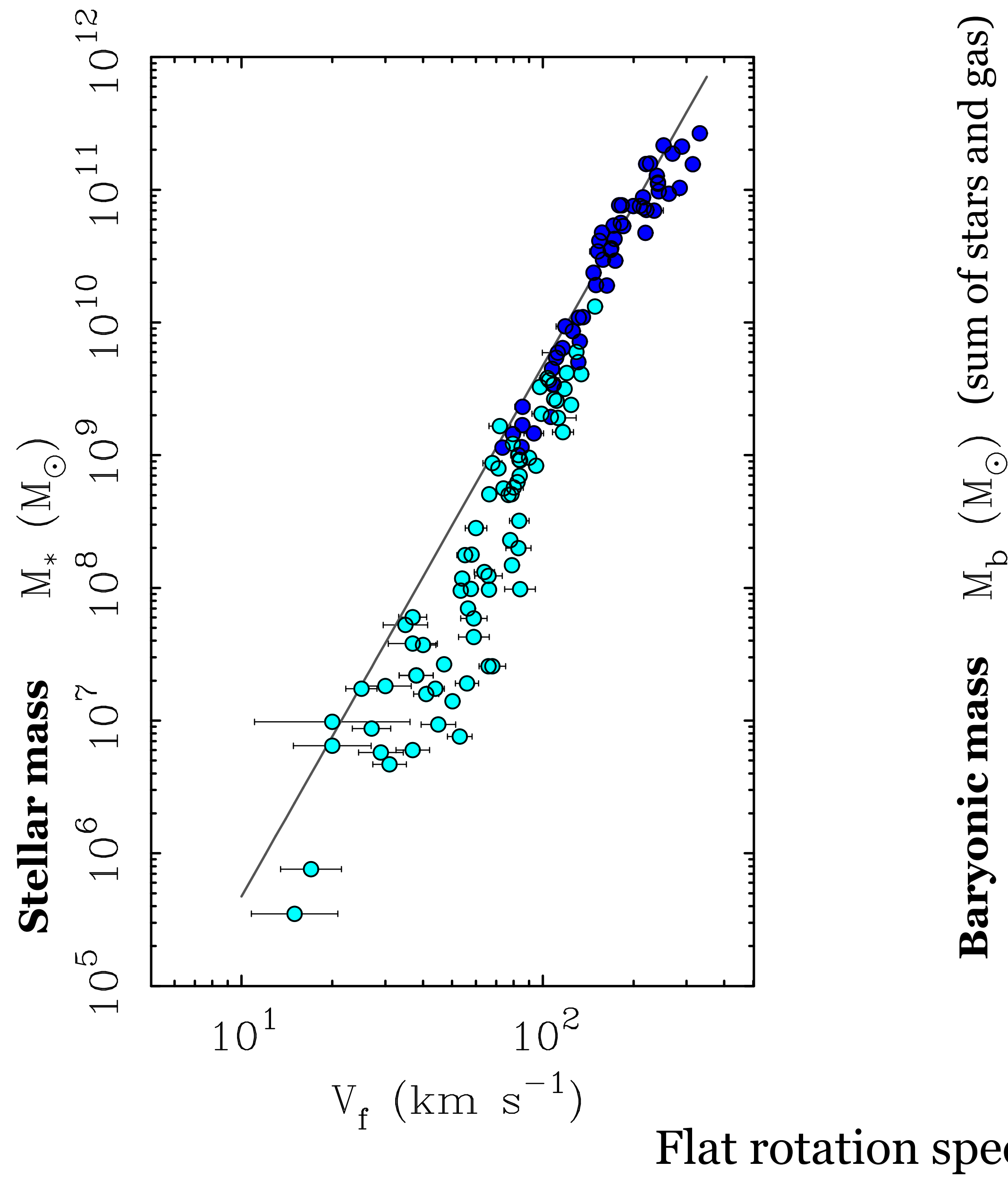


Low mass, gas dominated LSBs

# Tully-Fisher relations

amplitude of flat rotation correlates with mass

$$\frac{\sigma_D}{D} < 20\%$$



# Rotating galaxies

Fundamentally, Tully-Fisher is a relation between **baryonic mass** (stars+gas) and the amplitude of the **flat rotation speed**.

This is the  
**Baryonic Tully-Fisher Relation**

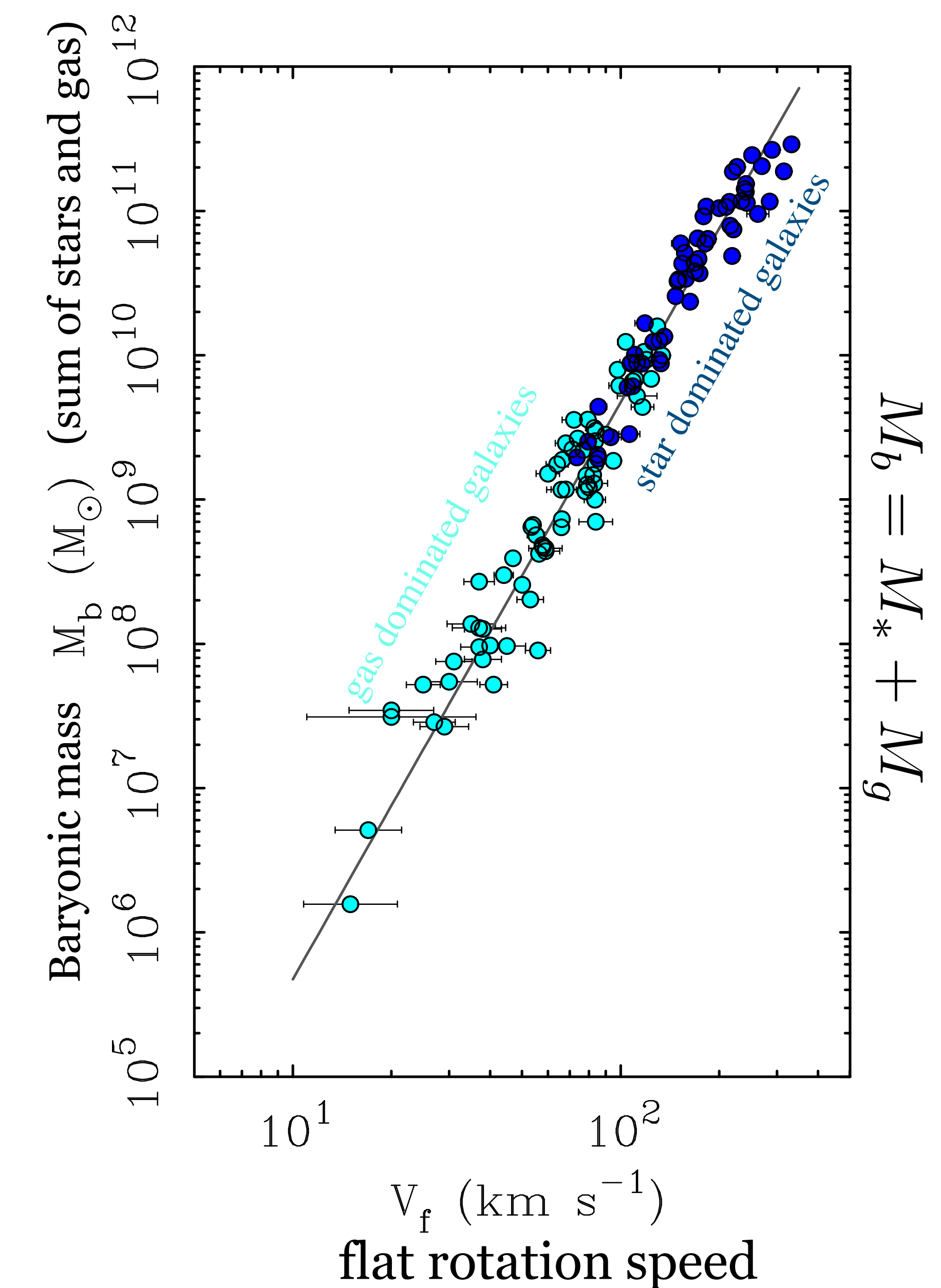
$$M_b = A V_f^4$$

$$A = 48.5 \pm 3.3 \text{ } M_{\odot} (\text{km s}^{-1})^{-4}$$

with remarkably little  
intrinsic scatter

$$\sigma < 0.11 \text{ dex}$$

This is about how much scatter we expect from stellar population mass-to-light variations, leaving very little room for other sources of scatter.



Example application:

Calibrate BTFR with 50 galaxies having distances that are known via either Cepheids or Tip of the Red Giant Branch measurements.

Applied to ~100 galaxies with high quality rotation curves, this provides a local measurement of the Hubble constant:

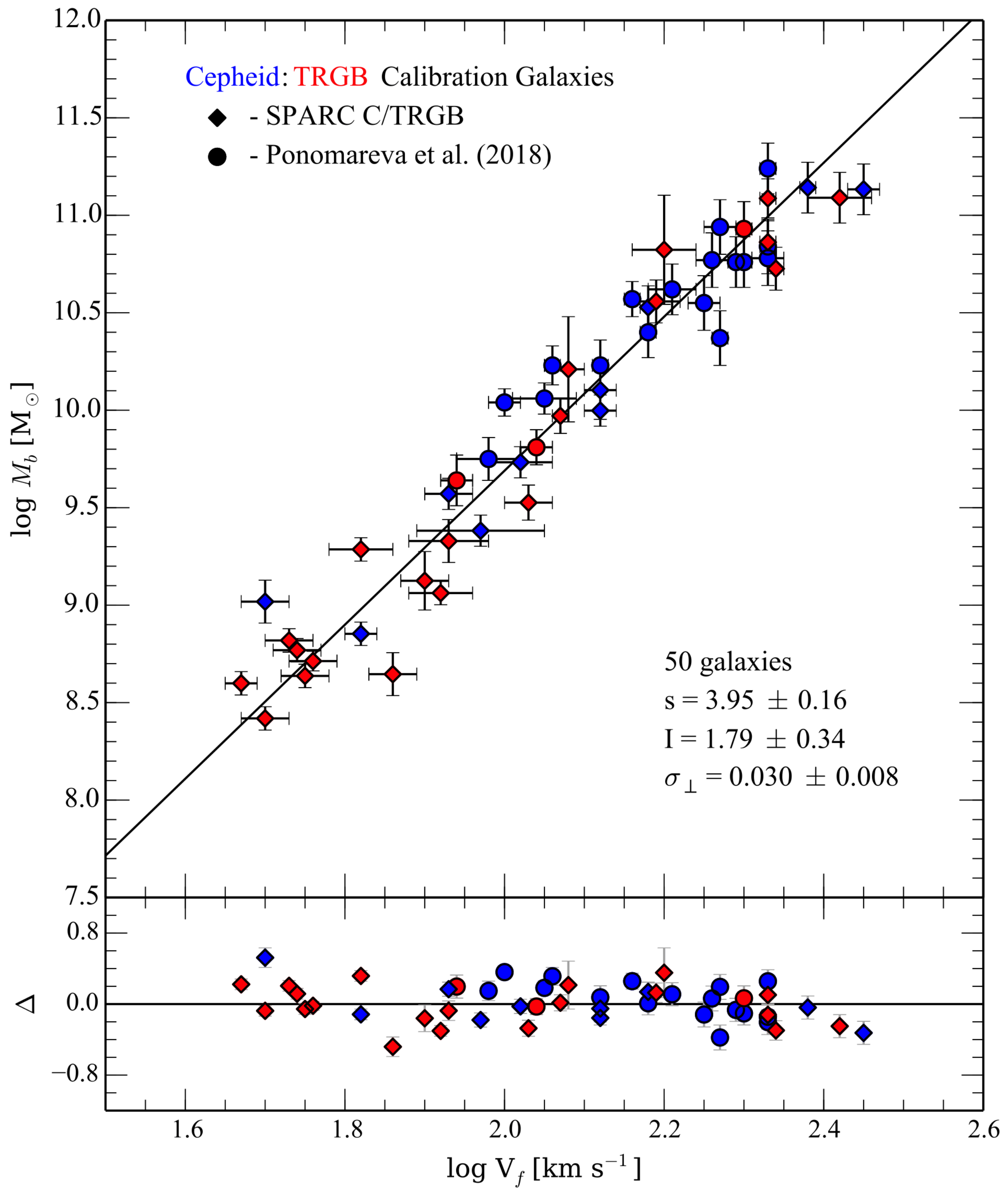
$$H_0 = 75.1 \pm 2.3 \text{ (stat)} \pm 1.5 \text{ (sys)} \text{ km s}^{-1} \text{ Mpc}^{-1}$$

Schombert, McGaugh, & Lelli 2020, AJ, 160, 71

This is consistent with the application of the traditional luminosity-line width Tully-Fisher relation to a much larger sample of ~10,000 galaxies.

$$H_0 = 75.1 \pm 0.2 \text{ (stat)} \pm 3 \text{ (sys)} \text{ km s}^{-1} \text{ Mpc}^{-1}$$

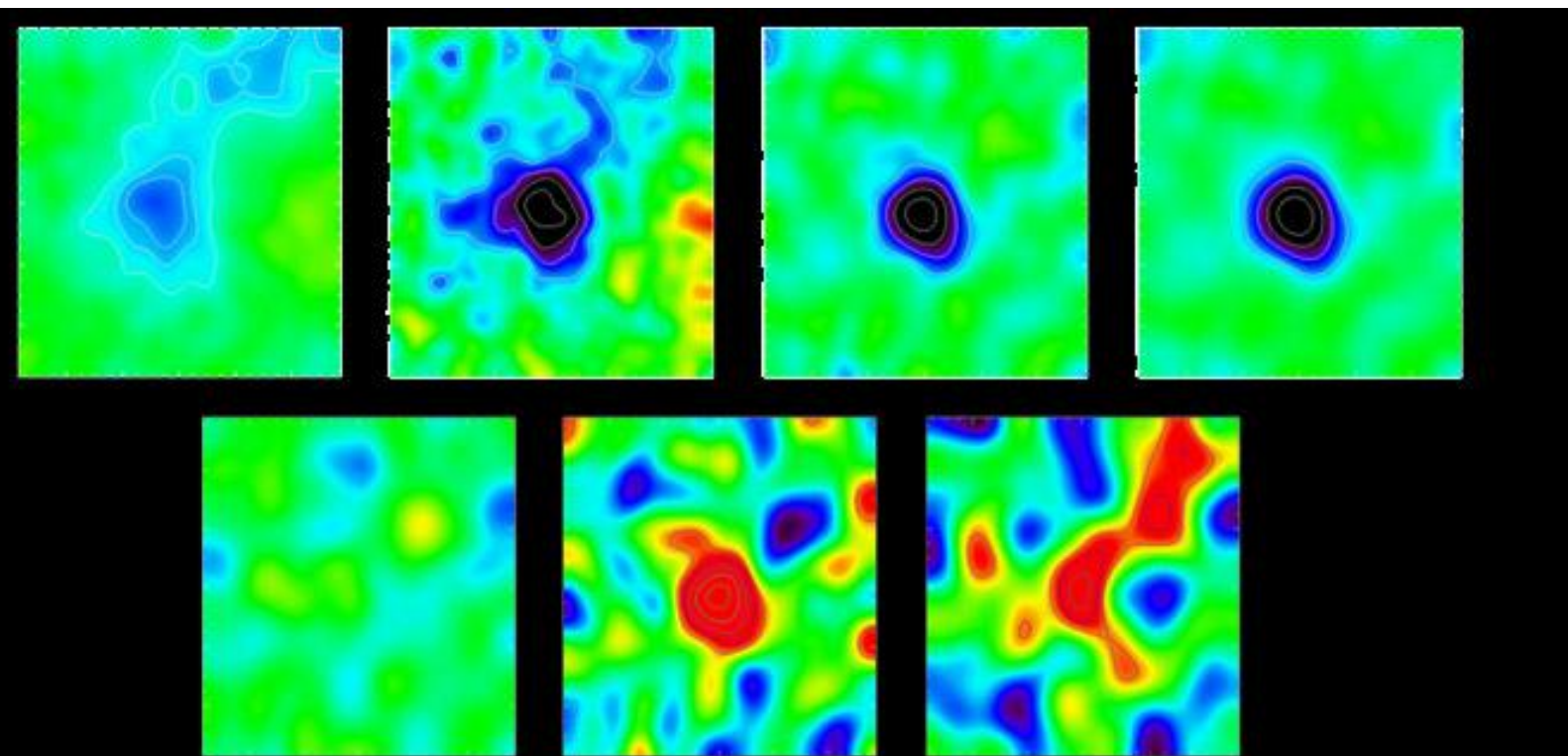
Kourkchi, Tully, *et al.* 2020, arXiv:2009.00733



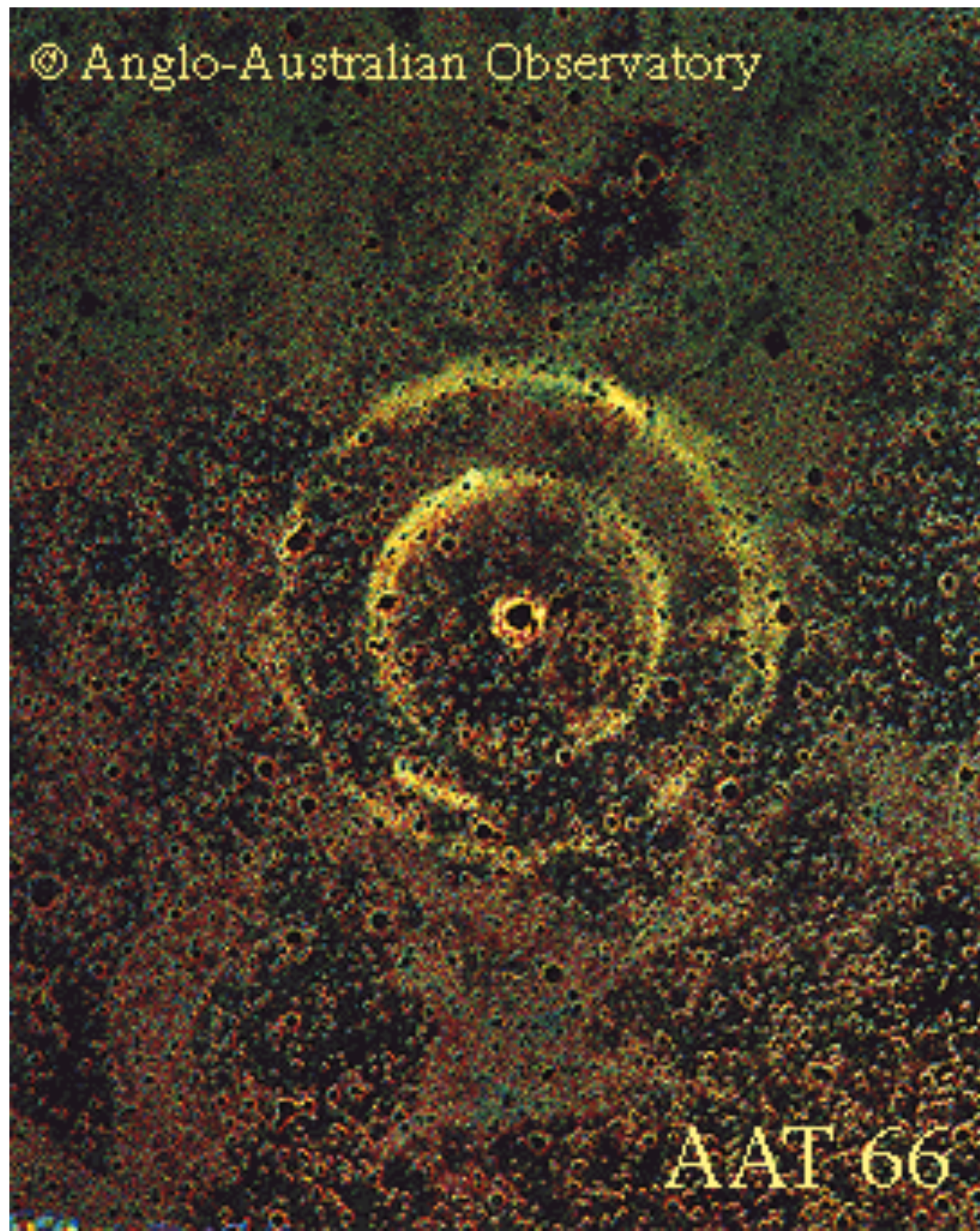
# Distance Scale

- Absolute Methods
  - Light echo
  - Gravitational lens time delay
  - Sunyaev-Zeldovich (SZ) effect
  - water masers

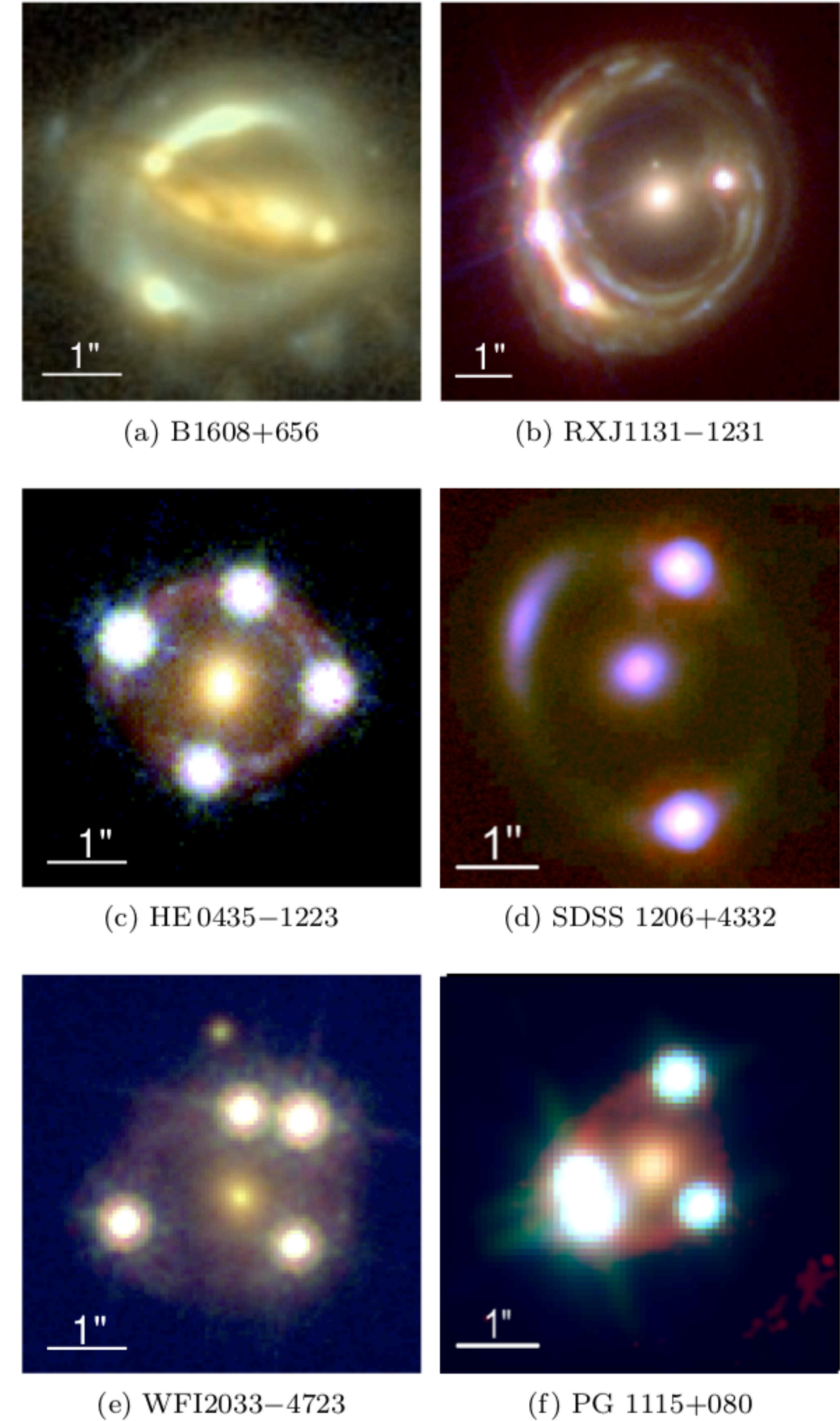
S-Z effect



Light echos



Gravitational Lenses



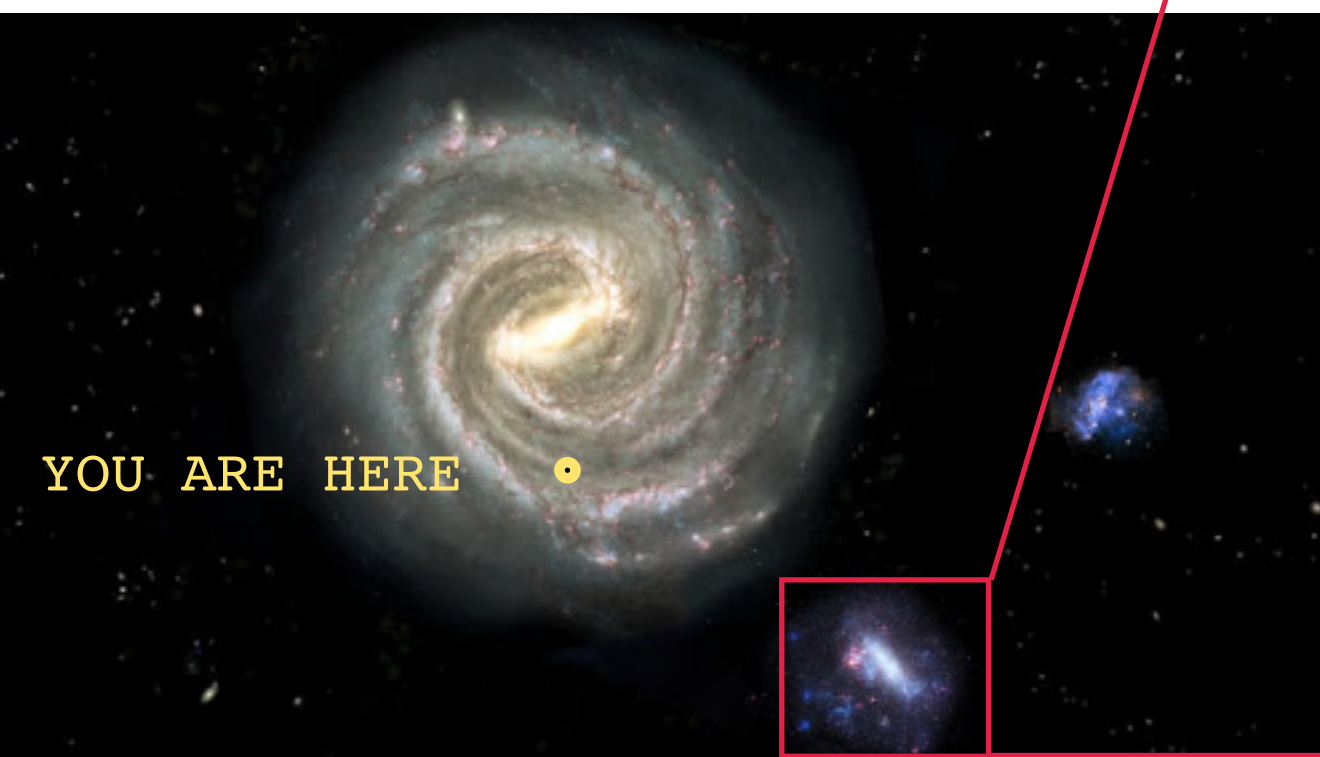
# Distance Scale

- Absolute Methods
  - Light echo
    - combines geometry & speed of light

Supernova 1987A occurred in the Large Magellanic Cloud, a satellite galaxy of the Milky Way.

The LMC is an important step in the distance ladder. The mean of over 200 measurements gives  $m - M = 18.49 \pm 0.13$  (49.9 kpc; Crandall & Ratra 2015).

Pietrzyński et al. (2019) model depth variations; find a mean LMC distance of  $\mu = 18.477 \pm 0.0263$  (49.6 kpc).



# Distance Scale

- Absolute Methods

- Light echo
  - combines geometry & speed of light

Flash of supernova seen directly, then seen reflected by encircling ring of dust with a time delay that depends on size, distance, and the speed of light.

time delays:

$$\Delta t_B = \frac{R_{\text{ring}}}{c} (1 - \sin i)$$

$$\Delta t_C = \frac{R_{\text{ring}}}{c} (1 + \sin i)$$

measured time delays:

$$\Delta t_B = 90 \text{ days}$$

$$\Delta t_C = 400 \text{ days}$$

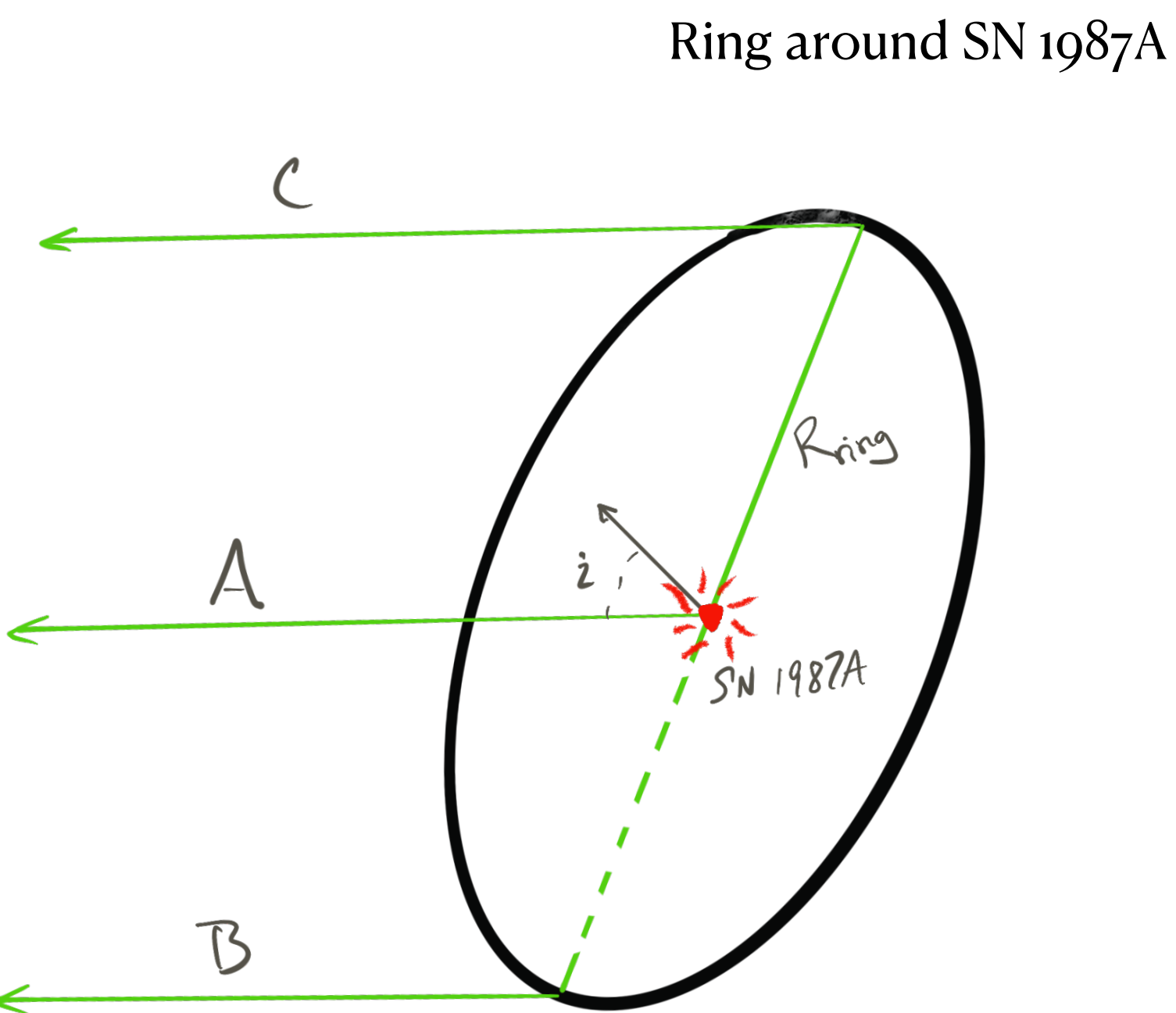
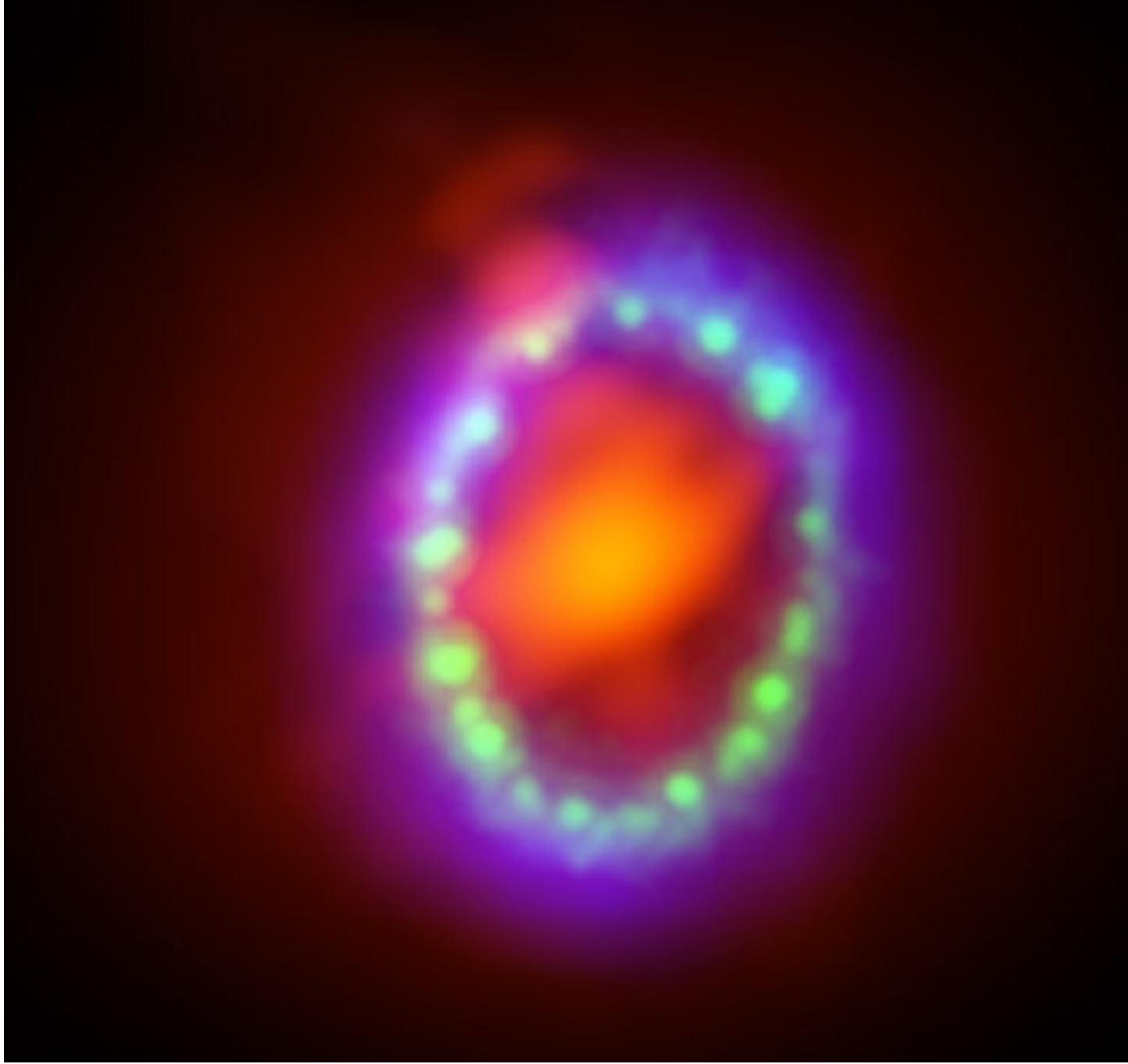
Two equations with two unknowns:

$$R_{\text{ring}} = 0.42 \pm 0.03 \text{ pc}$$

$$i = 43^\circ$$

Angular size of major axis  $\theta_{\text{ring}} = 1.66''$

$$\theta_{\text{ring}} = \frac{R_{\text{ring}}}{d_{\text{LMC}}} \rightarrow d_{\text{LMC}} = 51.9 \pm 3.1 \text{ kpc} \quad (\text{Crotts et al. 1995})$$



# Distance Scale

- Absolute Methods
  - Gravitational lens time delay

There is a delay between the arrival times of the multiple images that occur in gravitational lenses:

$$\Delta t_i = (1 + z_i) \left( \frac{1}{2c} \frac{D_L D_S}{D_{LS}} \alpha_i^2 - \frac{2}{c^3} \int \Phi(s) ds \right)$$

The time delay is tricky to measure, but in principle this gives a direct geometrical estimate of the distance: it's like parallax to cosmic distances, bypassing all the rungs in the distance ladder.

Can use distance-redshift relation to replace  $D_L(z_L)$  and  $D_S(z_S)$  with  $H_0$  and  $q_0$ .

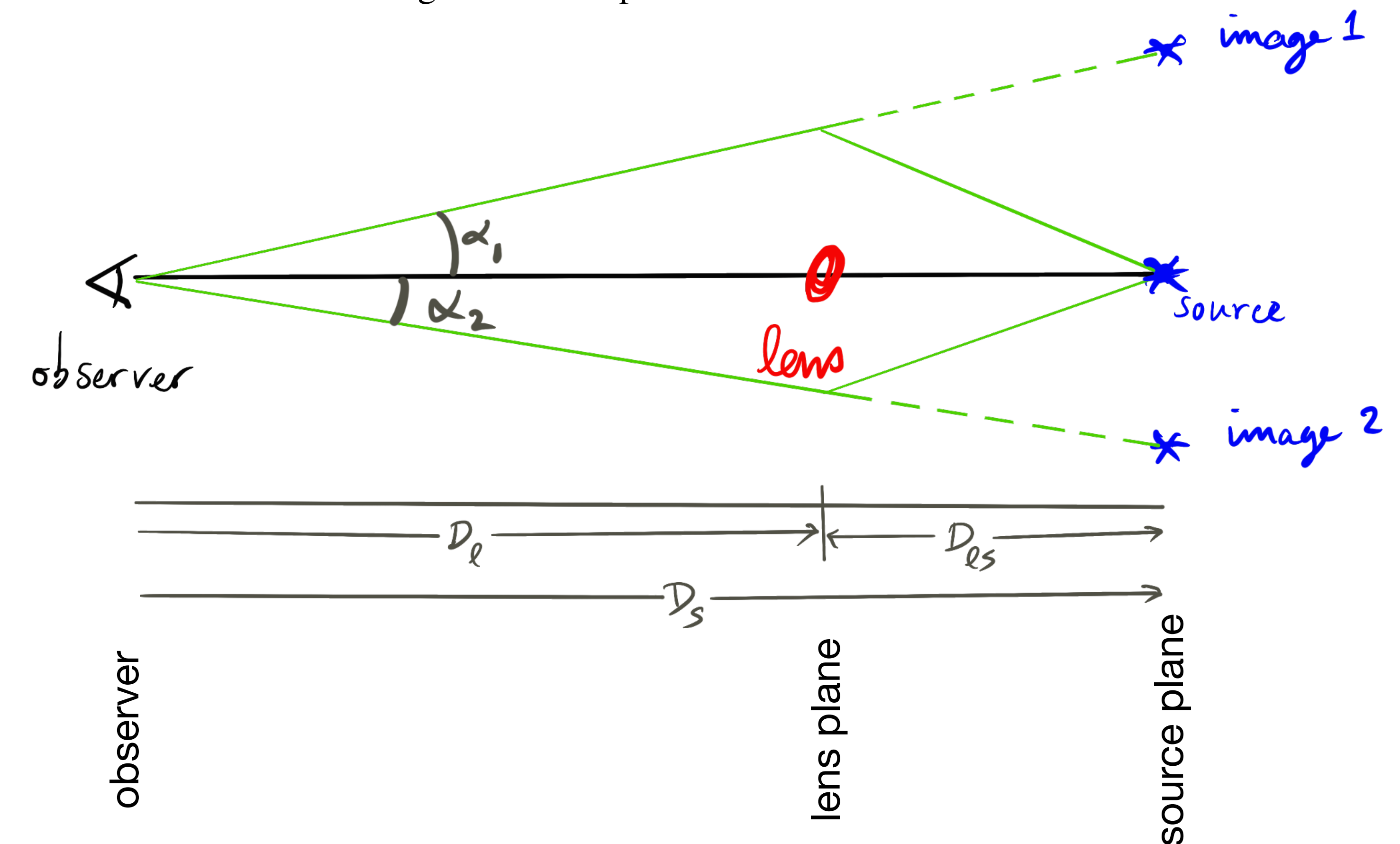
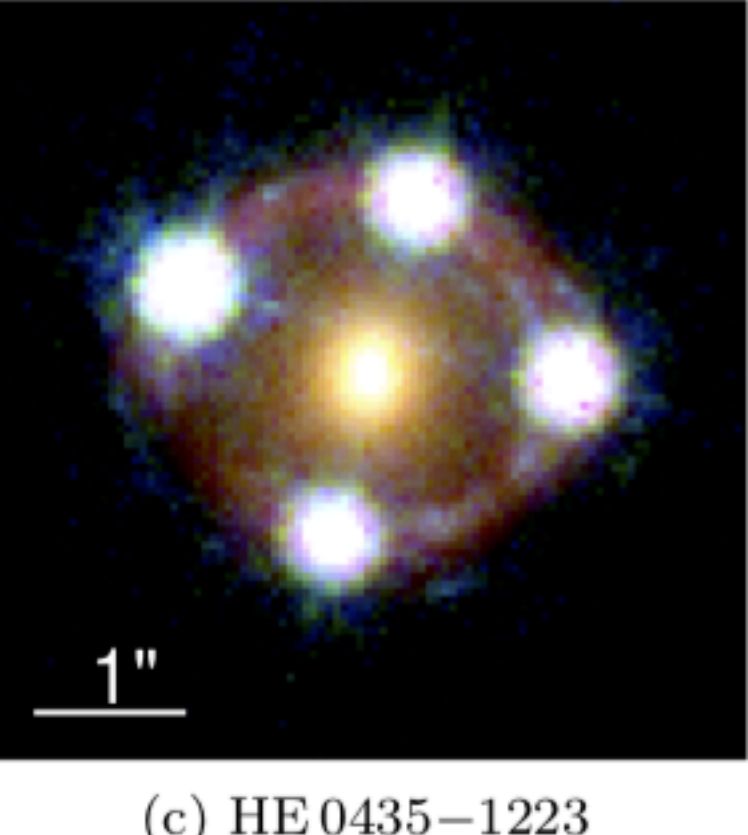
$D_L$  lens distance

$D_S$  source distance

$D_{LS}$  lens-source separation

$\alpha_i$  observed image-lens angle

$\Phi(s)$  gravitational potential of lens



# Distance Scale

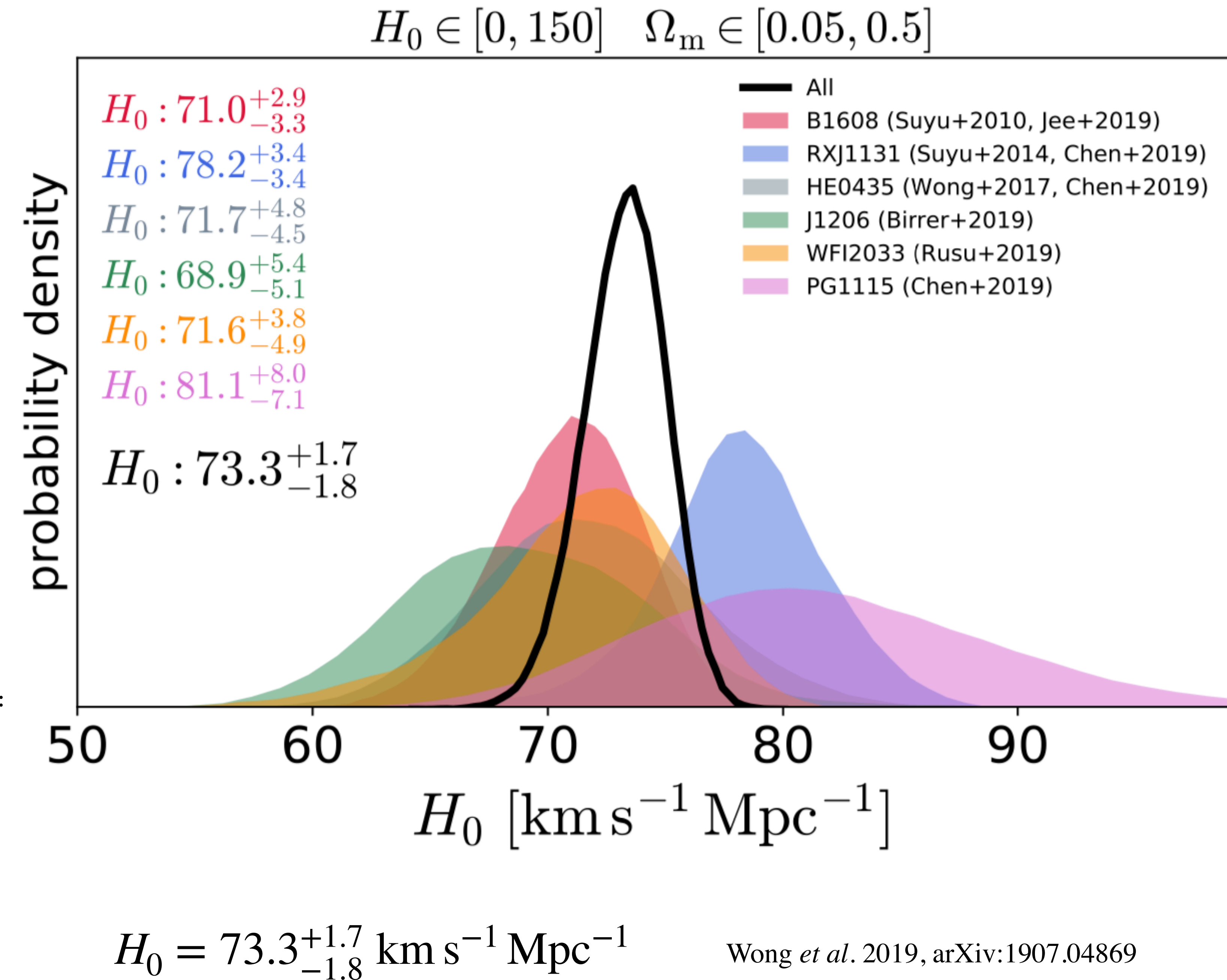
- Absolute Methods
  - Gravitational lens time delay

There is a delay between the arrival times of the multiple images that occur in gravitational lenses:

$$\Delta t_i = (1 + z_i) \left( \frac{1}{2c} \frac{D_L D_S}{D_{LS}} \alpha_i^2 - \frac{2}{c^3} \int \Phi(s) ds \right)$$

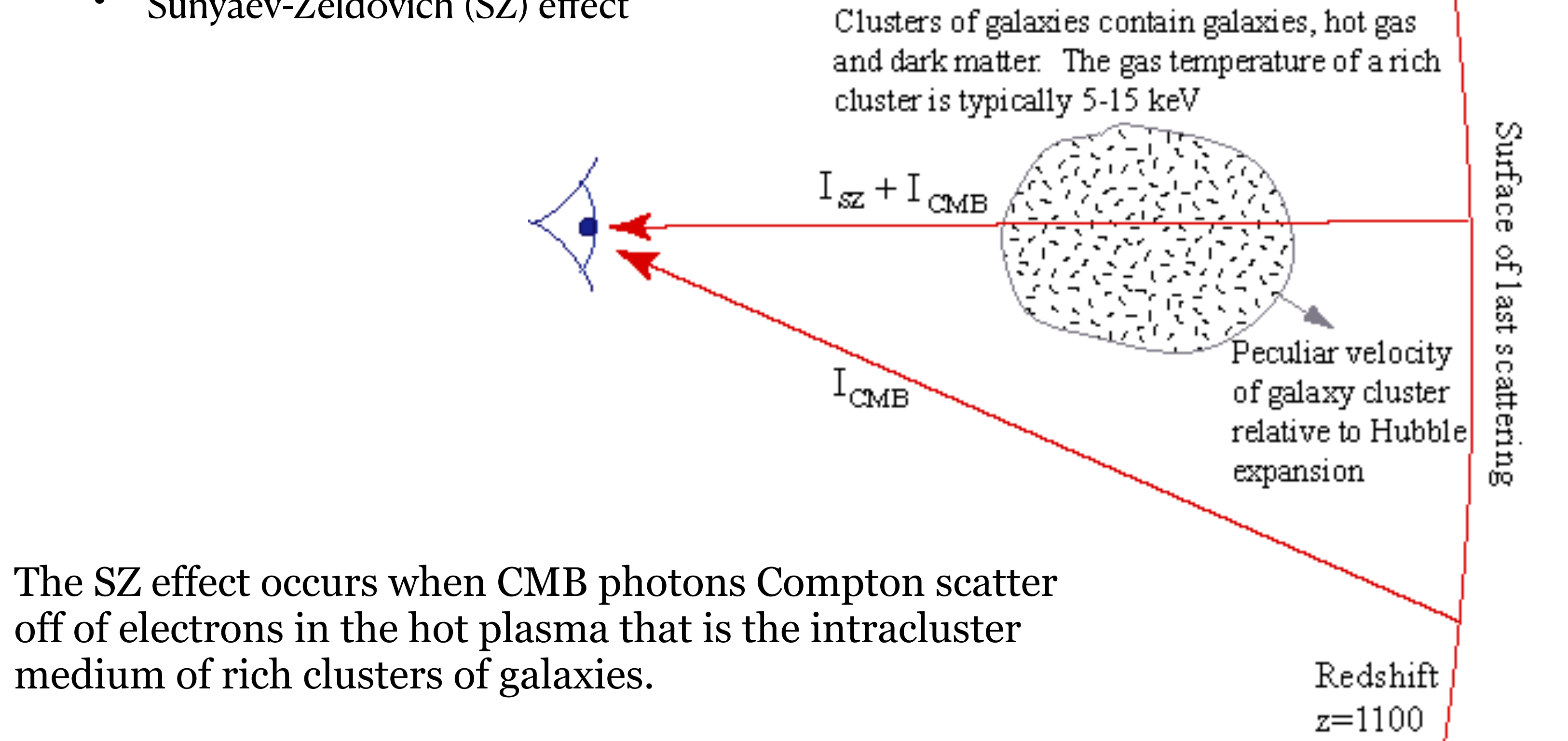
The time delay is tricky to measure, but in principle this gives a direct geometrical estimate of the distance: it's like parallax to cosmic distances, bypassing all the rungs in the distance ladder.

Can use distance-redshift relation to replace  $D_L(z_L)$  and  $D_S(z_S)$  with  $H_0$  and  $q_0$ .

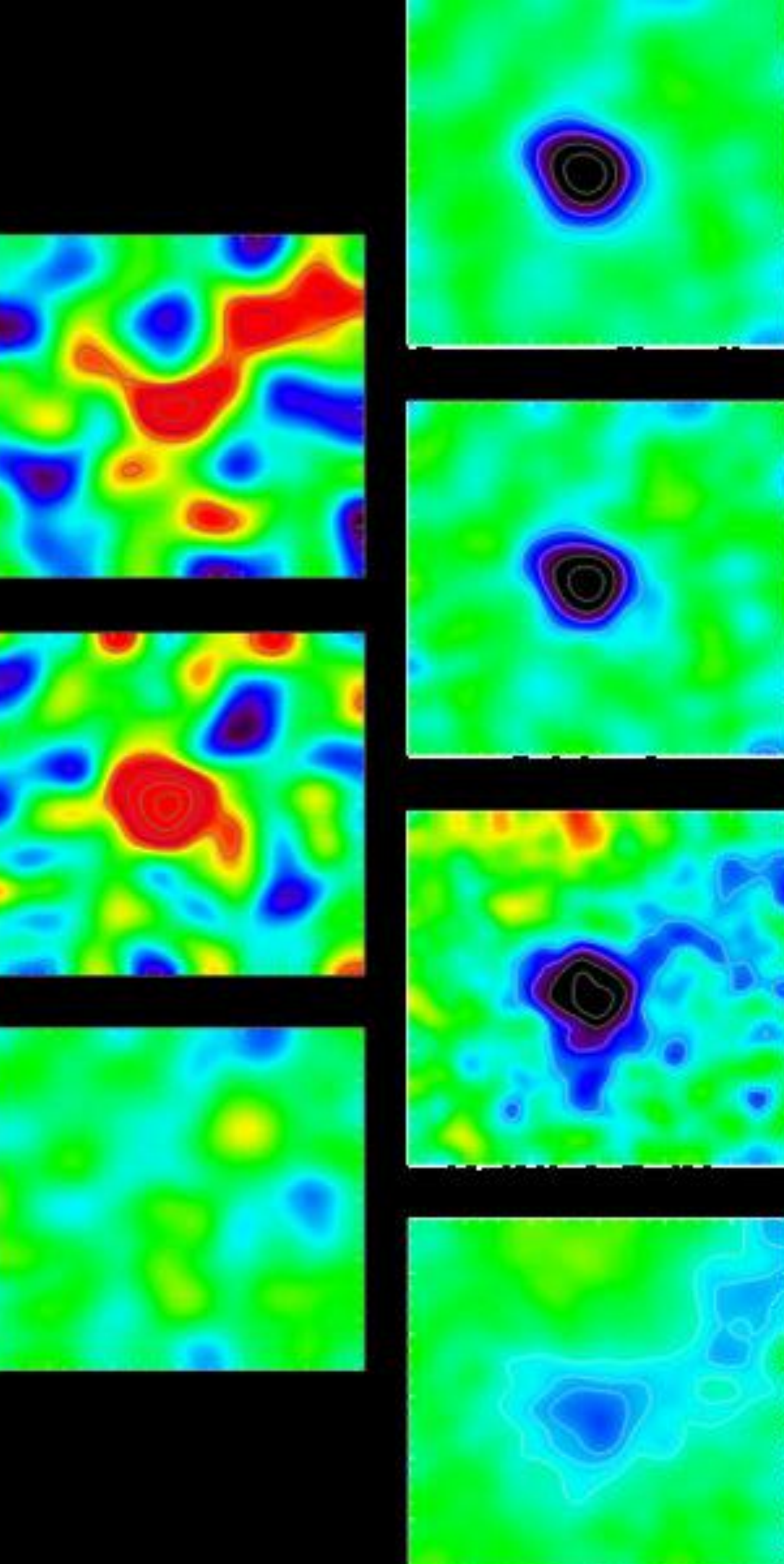


# Distance Scale

- Absolute Methods
  - Sunyaev-Zeldovich (SZ) effect

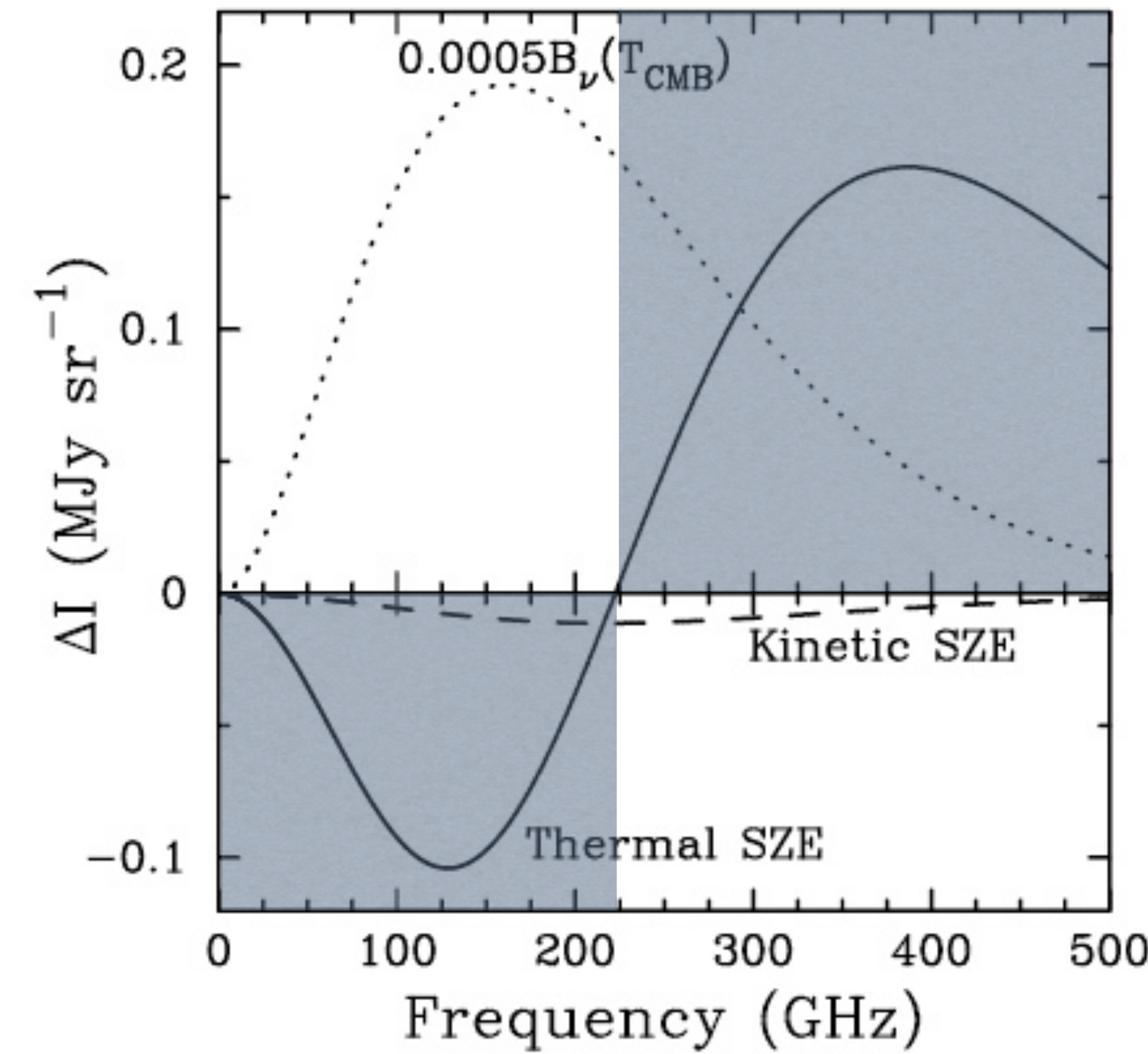
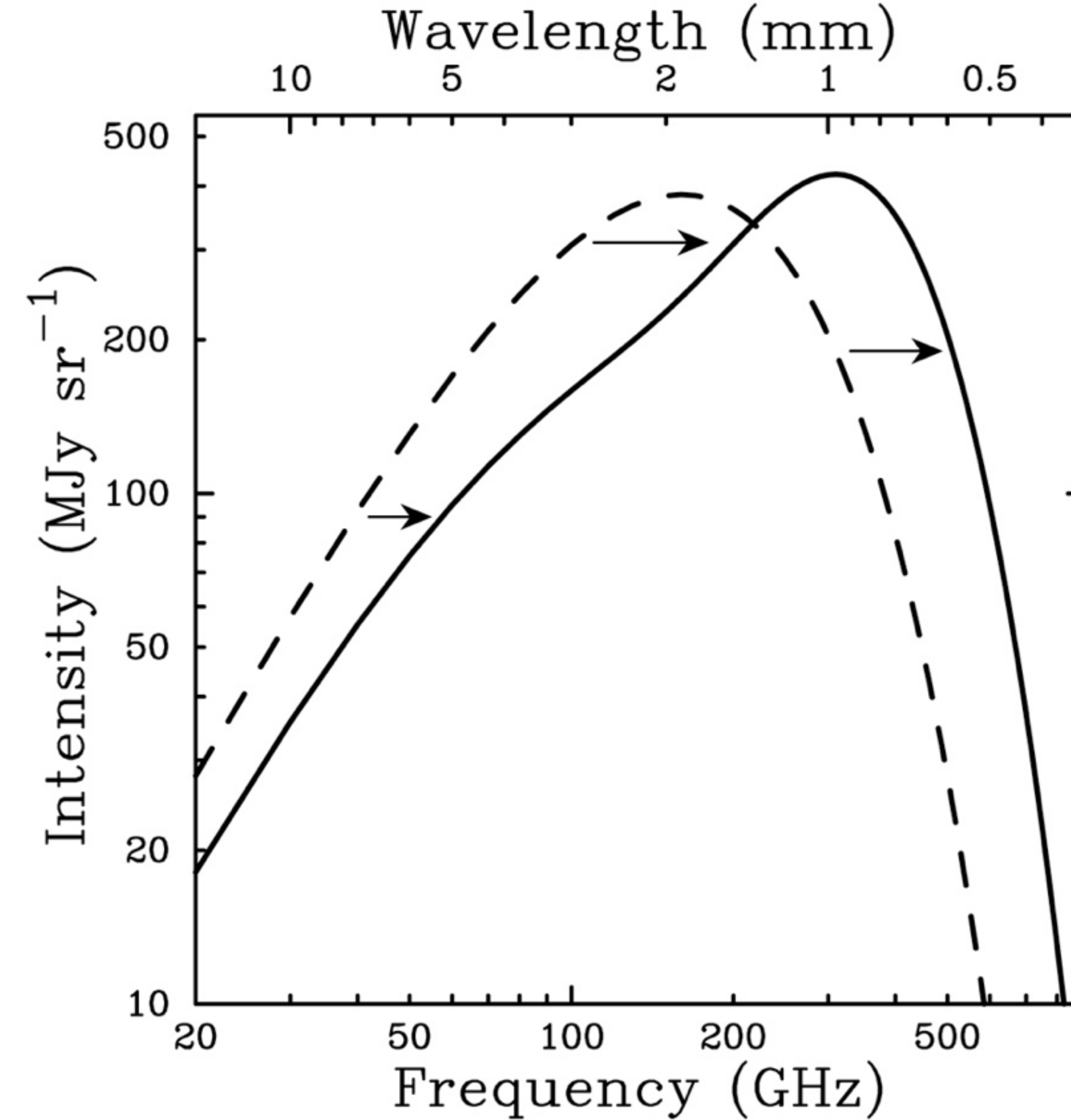


The SZ effect occurs when CMB photons Compton scatter off of electrons in the hot plasma that is the intracluster medium of rich clusters of galaxies.



The SZ effect occurs when CMB photons Compton scatter off of electrons in the hot plasma that is the intracluster medium of rich clusters of galaxies. Results in a net increase in the effective radiation Temperature.

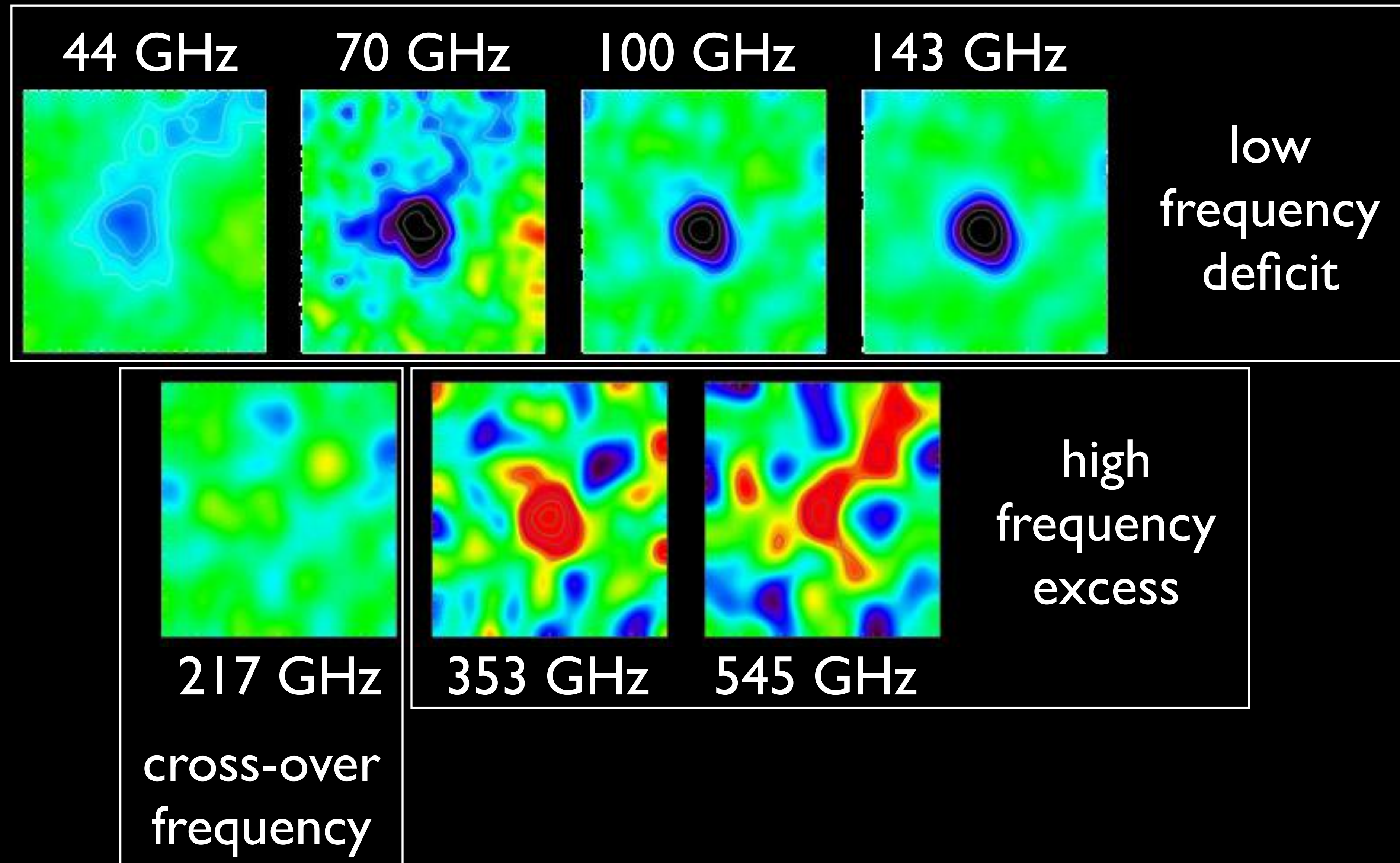
intensity  
boosted



intensity  
depleted

# SUNYAEV-ZEL'DOVICH EFFECT

detected by Planck



# Distance Scale

- Absolute Methods

- Sunyaev-Zeldovich (SZ) effect

Cluster optical depth  $\tau_{SZ} = 2\sigma_T n_e R_c$  where  
 $\sigma_T$  is the Thomson scattering cross-section,  $n_e$  is the electron density, and  $R_c$  is the cluster radius.

The X-ray flux is  $f_X = \frac{4\pi}{3} \frac{R_c^3 \epsilon(\nu)}{4\pi D^2}$

where the Bremsstrahlung emissivity is  $\epsilon(\nu) = A n_e^2 T_X^{1/2} e^{-\frac{h\nu}{kT_X}}$

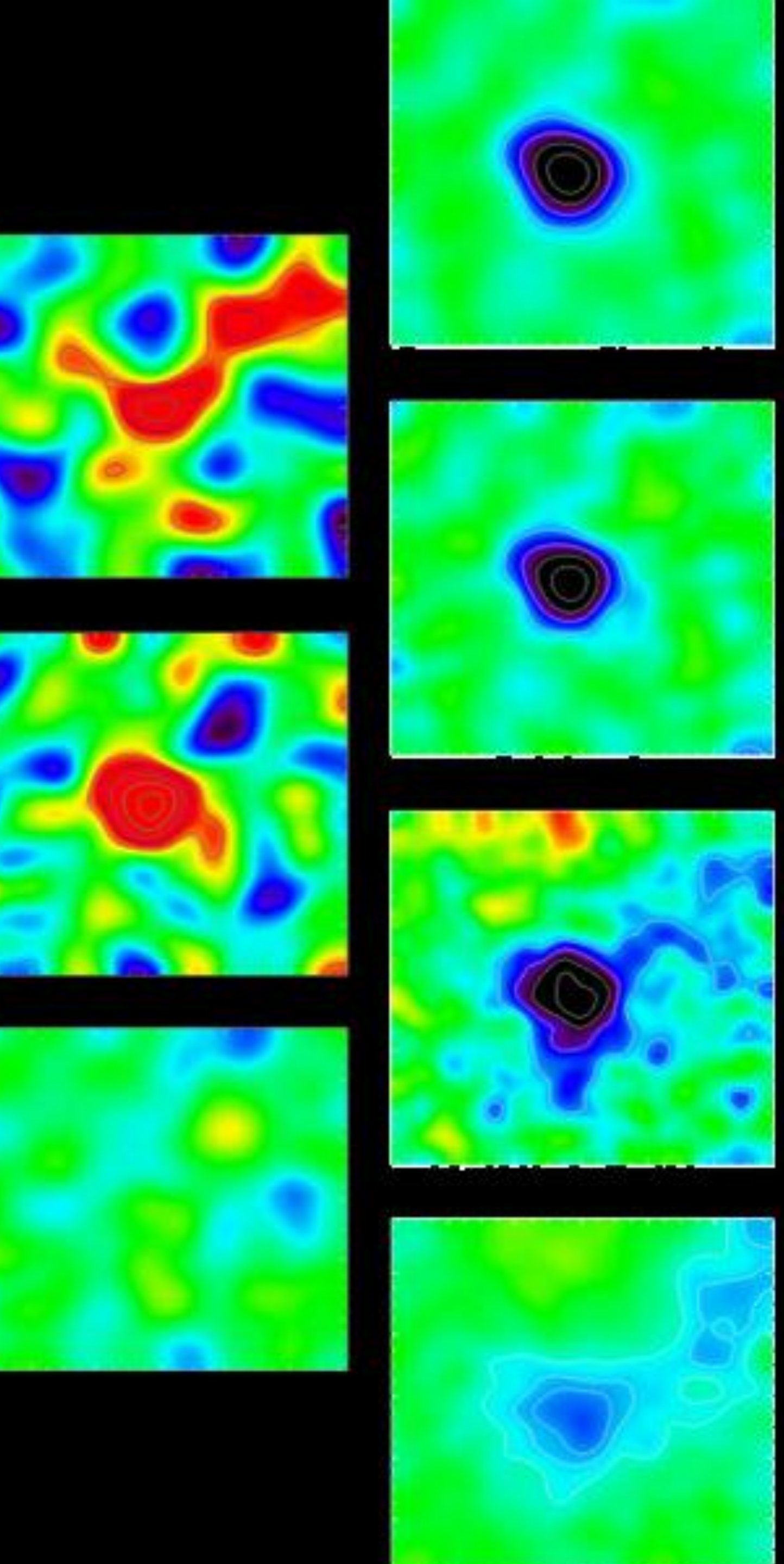
All of which can be combined to give the distance

$$D = \frac{A}{24\sigma_T} \frac{e^{-\frac{h\nu}{kT_X}}}{\sqrt{T_X}} \frac{\theta_X}{f_X} \frac{\tau_{SZ}^2}{(1+z)^2}$$

by equating the angular diameter  $\theta_X$  with the path length  $2R_c$  experienced by the CMB photons

$$H_0 = 69 \pm 8 \text{ km s}^{-1} \text{ Mpc}^{-1}$$

Schmidt *et al.* 2004

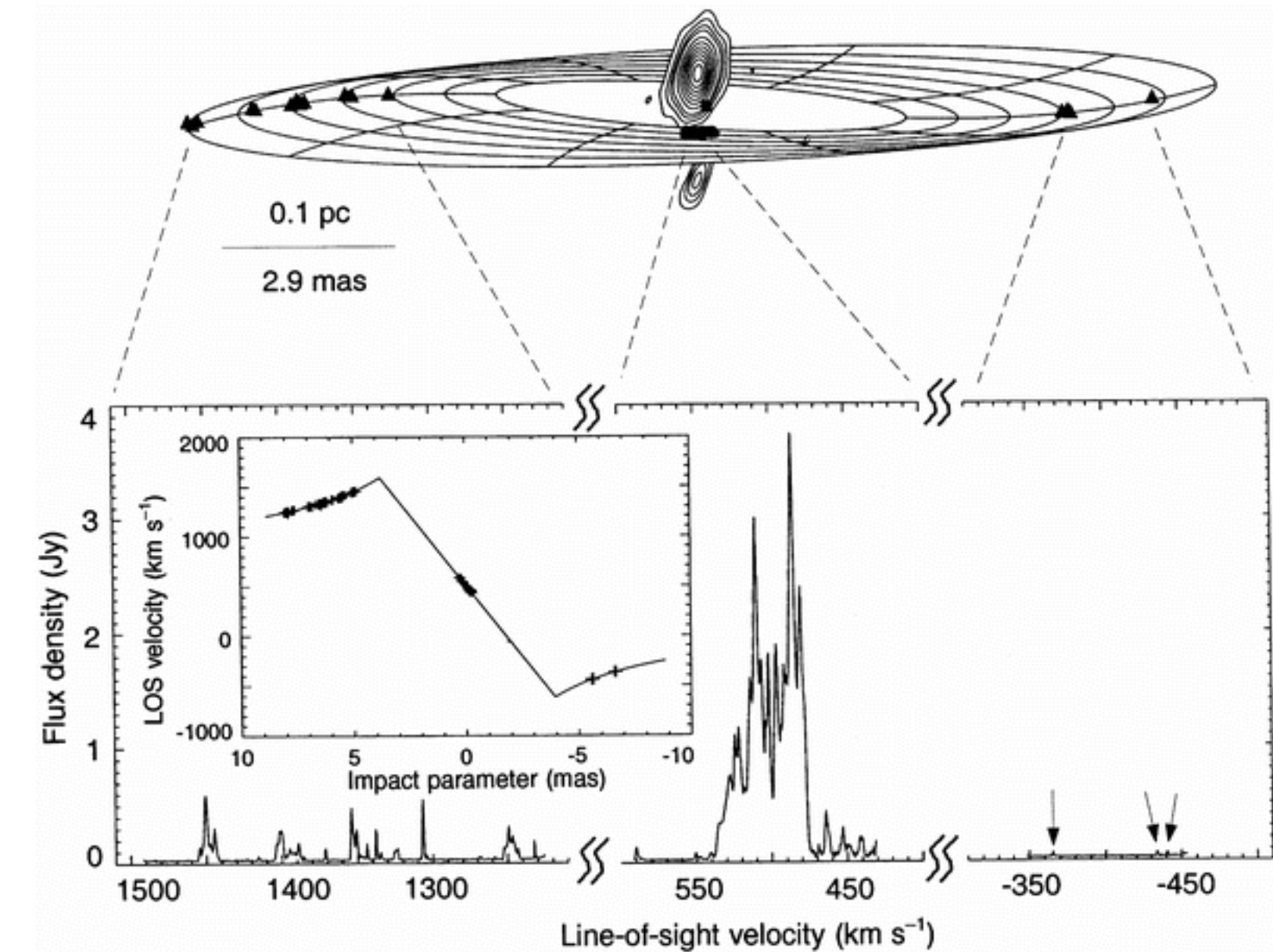


# Distance Scale

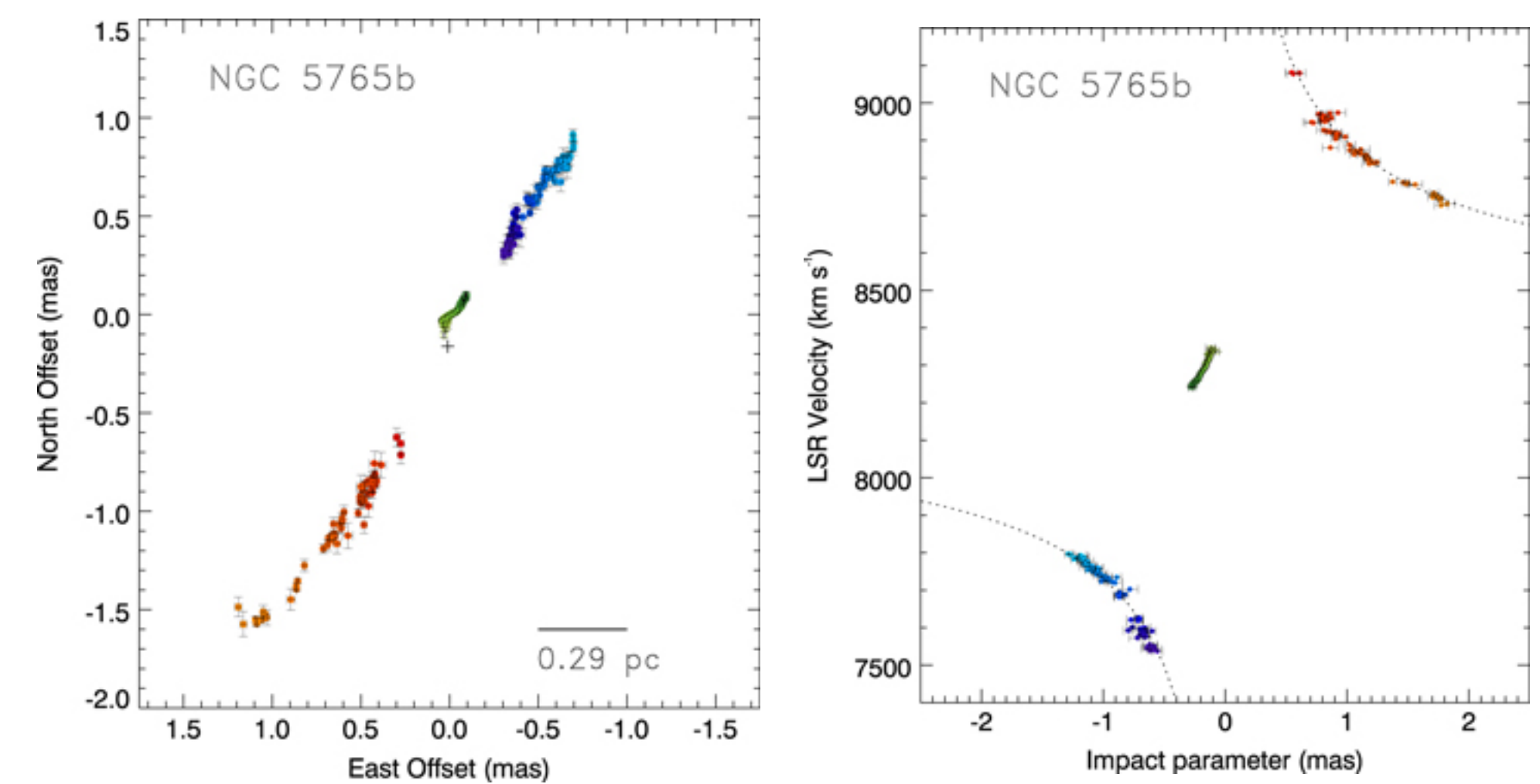
- Absolute Methods
  - water masers

Conditions in the ISM are sometimes right to produce masers - the amplification of molecular lines due to level inversion, e.g., H<sub>2</sub>O at 1.35 cm.

Sometimes found orbiting the central supermassive black holes of nearby galaxies. Can watch them orbit by tracking their positions with VLBI (proper motions at microarcsecond accuracy). Can also measure their radial velocities via the Doppler effect. We understand orbits around point masses, so these all combine to provide a geometric distance measurement that is independent of other rungs in the distance ladder.



NGC 5765 (Gao et al 2016)



The dotted line shows the best-fit Keplerian rotation curve assuming an edge-on thin-disk model without disk warping. This model gives an enclosed mass of  $4.4 \pm 0.44 \times 10^7 M_\odot$  and a recession velocity of 8304 km s<sup>-1</sup>.

# Distance Scale

- Absolute Methods
  - water masers

Herrnstein et al (1999) detect accelerations as well as velocities:

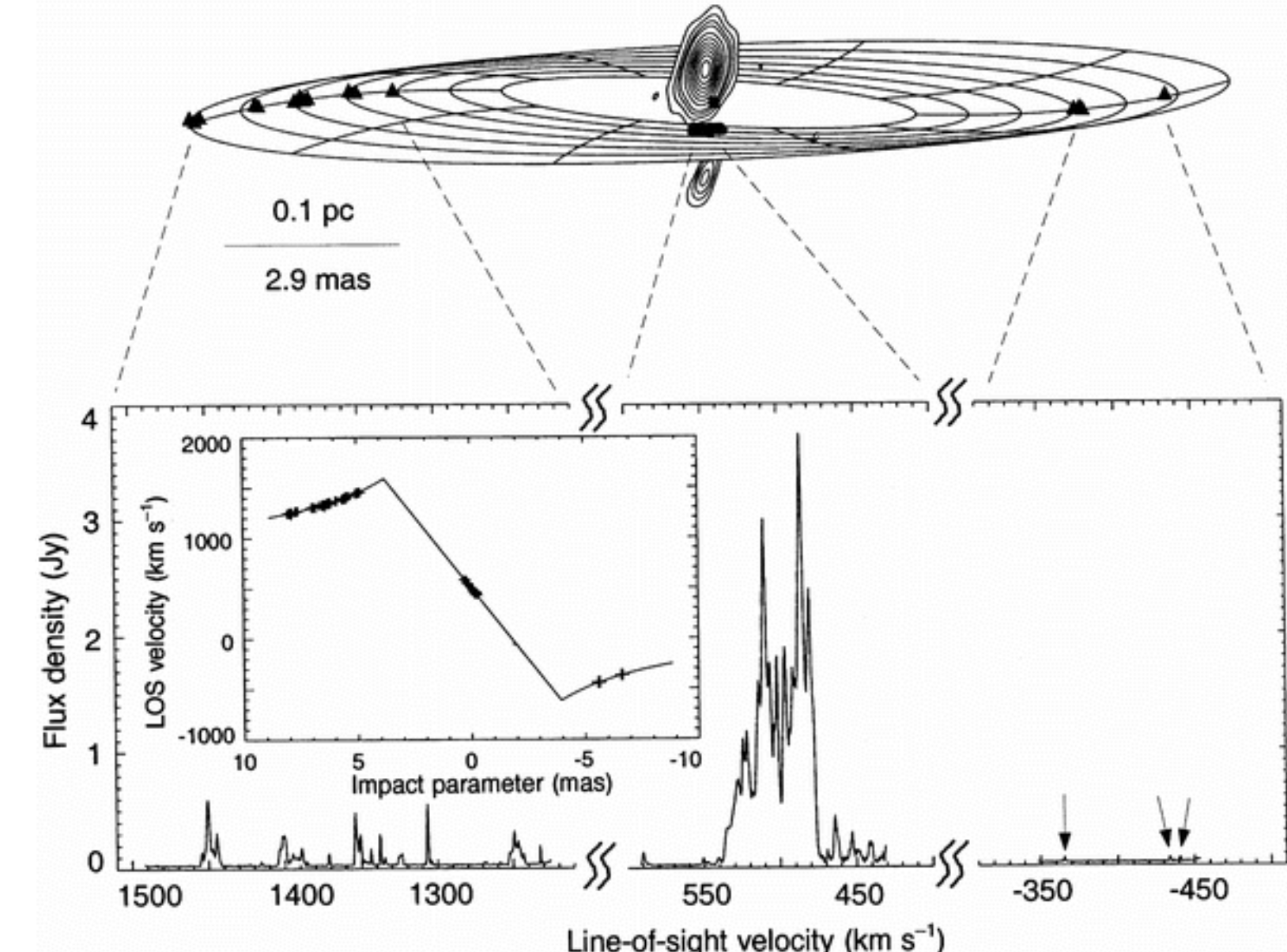
To convert the maser proper motions and accelerations into a geometric distance, we express  $\langle \dot{\theta}_x \rangle$  and  $\langle \dot{v}_{\text{LOS}} \rangle$  in terms of the distance and four disk parameters:

$$\langle \dot{\theta}_x \rangle = 31.5 \left[ \frac{D_6}{7.2} \right]^{-1} \left[ \frac{\Omega_s}{282} \right]^{1/3} \left[ \frac{M_{7.2}}{3.9} \right]^{1/3} \left[ \frac{\sin i_s}{\sin 82.3^\circ} \right]^{-1} \left[ \frac{\cos \alpha_s}{\cos 80^\circ} \right] \mu\text{as yr}^{-1} \quad (1)$$

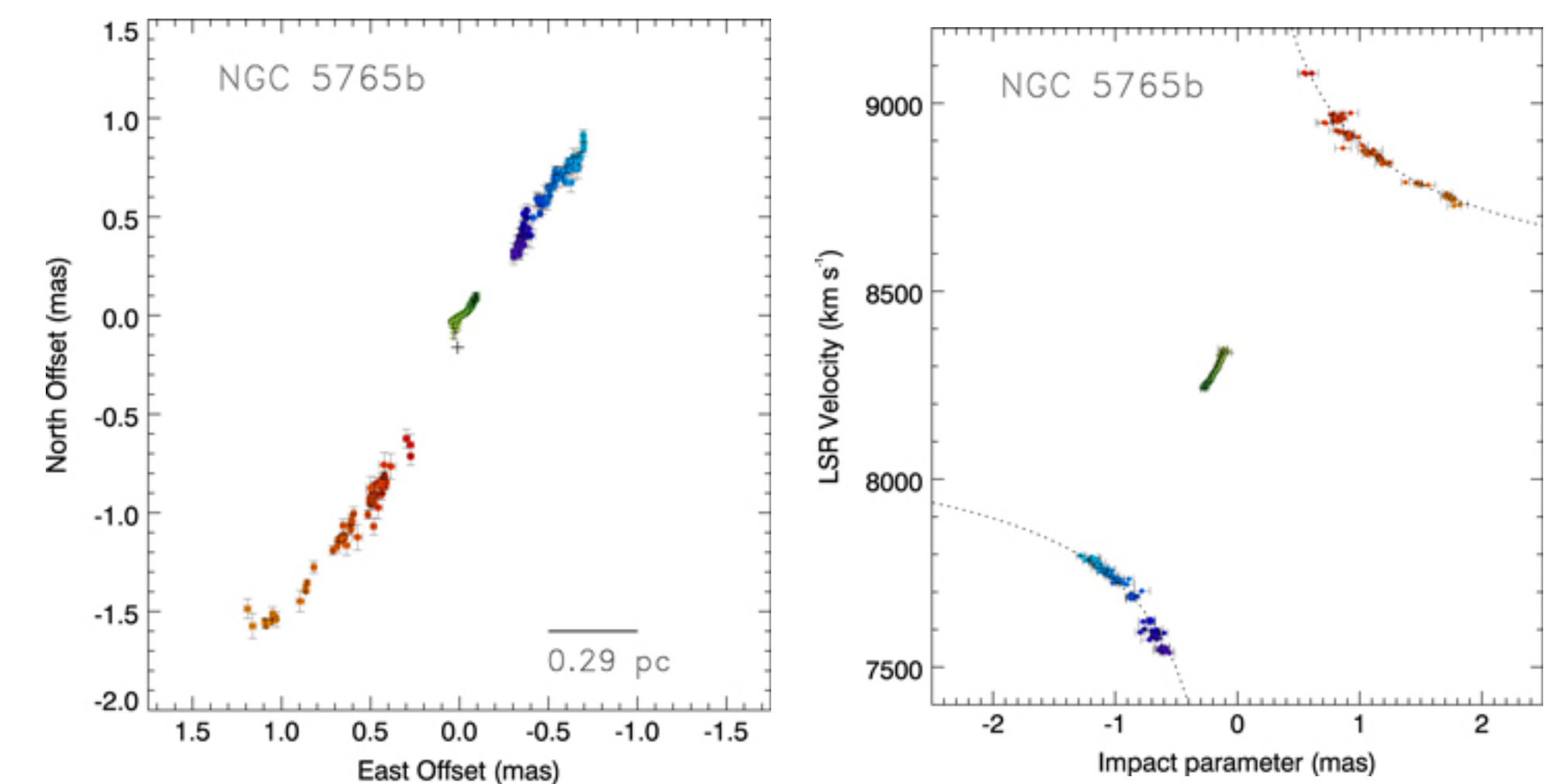
and

$$\langle \dot{v}_{\text{LOS}} \rangle = 9.2 \left[ \frac{D_6}{7.2} \right]^{-1} \left[ \frac{\Omega_s}{282} \right]^{4/3} \left[ \frac{M_{7.2}}{3.9} \right]^{1/3} \left[ \frac{\sin i_s}{\sin 82.3^\circ} \right]^{-1} \text{ km s}^{-1} \text{ yr}^{-1} \quad (2)$$

Here  $D_6$  is the distance in Mpc,  $\alpha_s$  is the disk position angle (East of North) at  $\langle r_s \rangle$ , and  $M_{7.2}$  is  $M/D \sin^2 i_s$  as derived from the high-velocity rotation curve and evaluated at  $D = 7.2$  Mpc and  $i_s = 82.3^\circ$  (in units of  $10^7 M_\odot$ ).  $\Omega_s \equiv (GM_{7.2}/\langle r_s \rangle^3)^{1/2}$  is the projected disk angular velocity at  $\langle r_s \rangle$  as determined by the slope of the systemic position–velocity gradient (in units of  $\text{km s}^{-1} \text{ mas}^{-1}$ ; see Fig. 1). In the denominators of each of the terms of equations (1) and (2), we include *a priori* estimates for each of these disk parameters, derived directly from the positions and velocities of the masers.

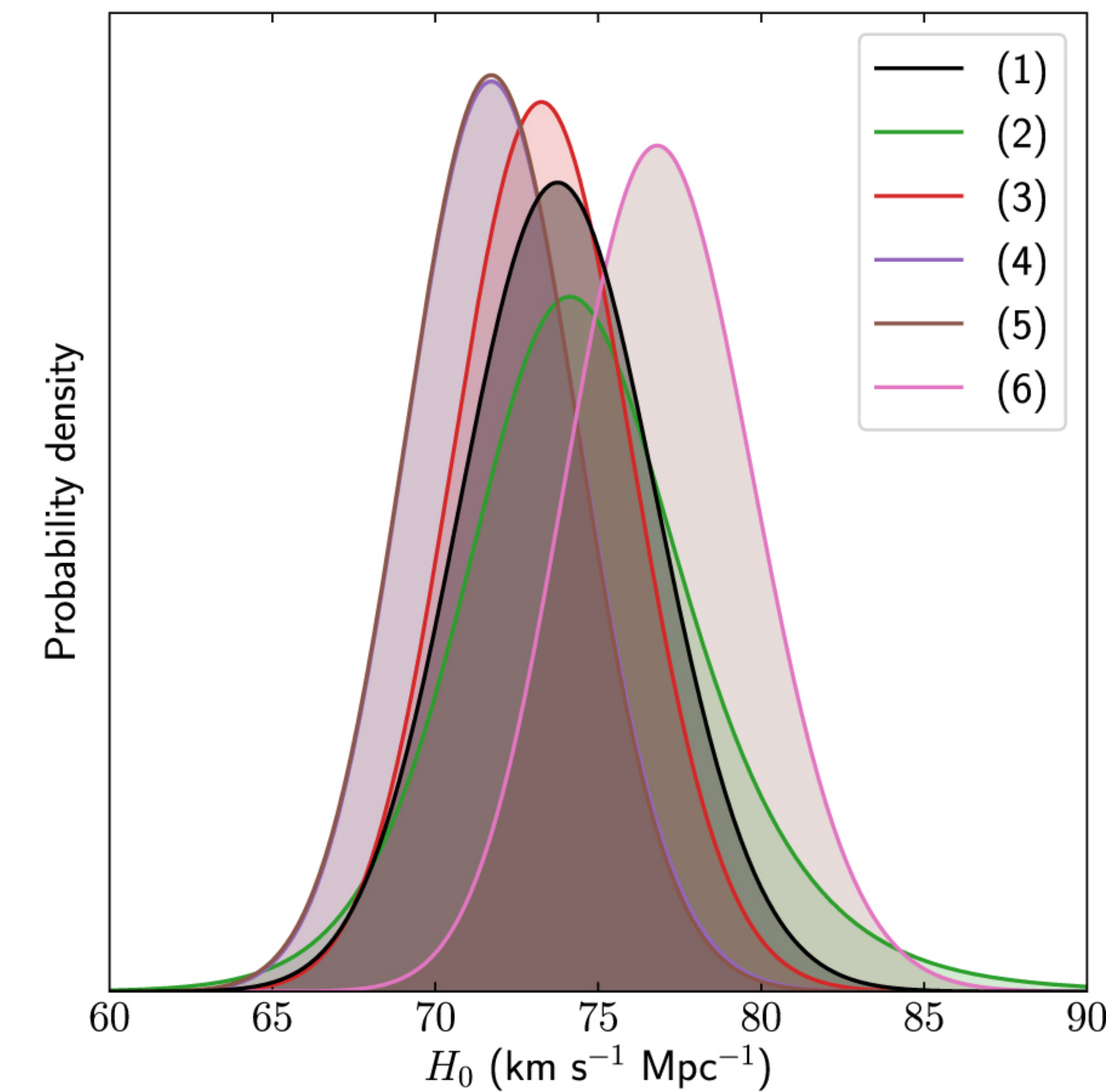
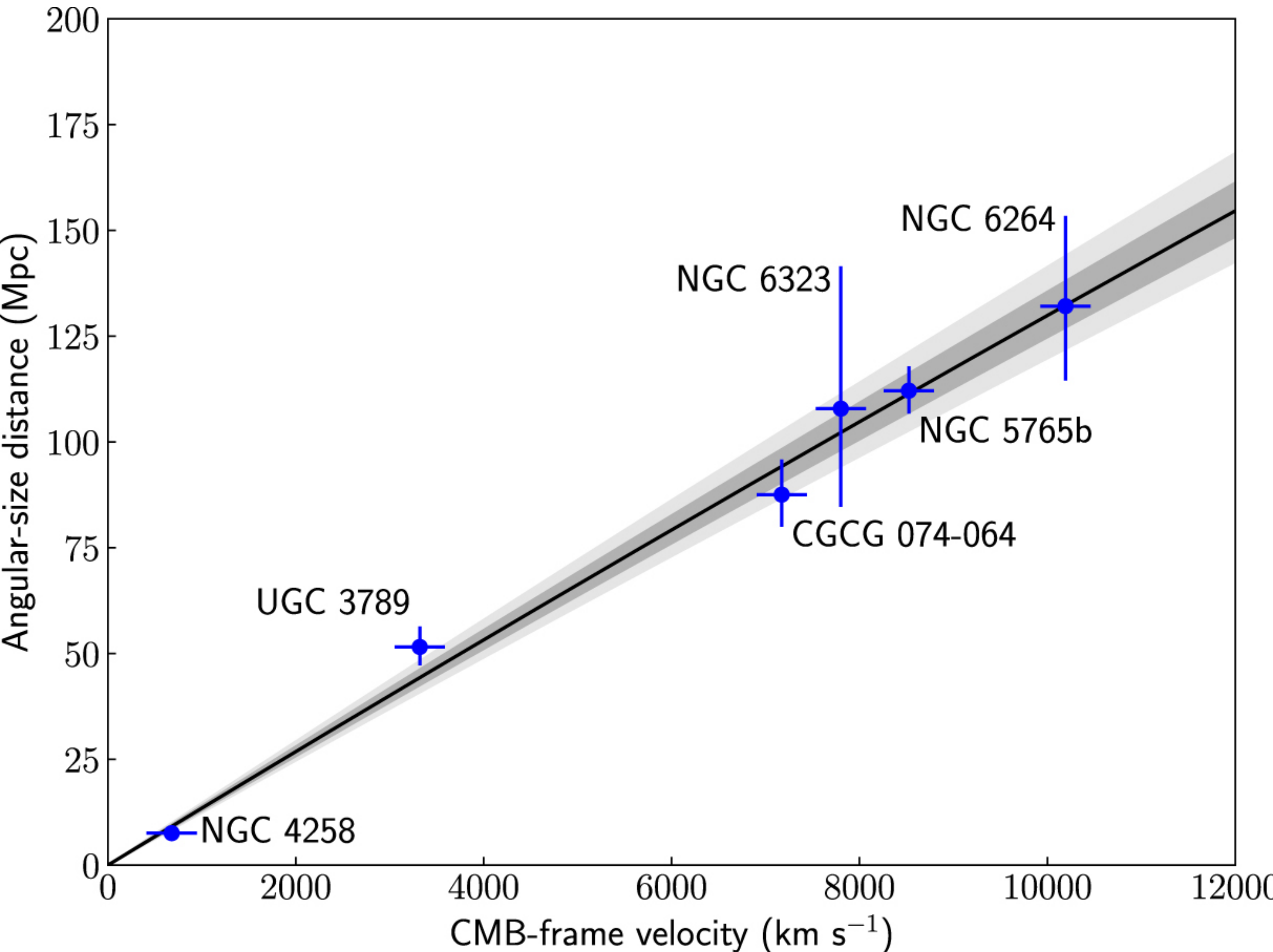


NGC 4258 (Herrnstein et al 1999)



The dotted line shows the best-fit Keplerian rotation curve assuming an edge-on thin-disk model without disk warping. This model gives an enclosed mass of  $4.4 \pm 0.44 \times 10^7 M_\odot$  and a recession velocity of  $8304 \text{ km s}^{-1}$ .

Megamaser Cosmology Project. XIII (Pesce et al. 2020)



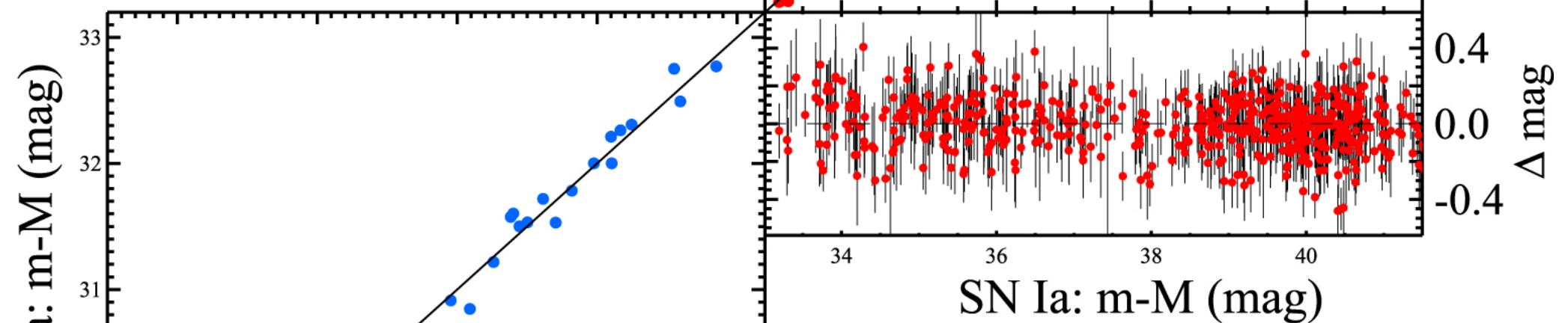
$$H_0 = 73.9 \pm 3.0 \text{ km s}^{-1} \text{ Mpc}^{-1}$$

# Continuity of distance scale ladder over 37 mag.

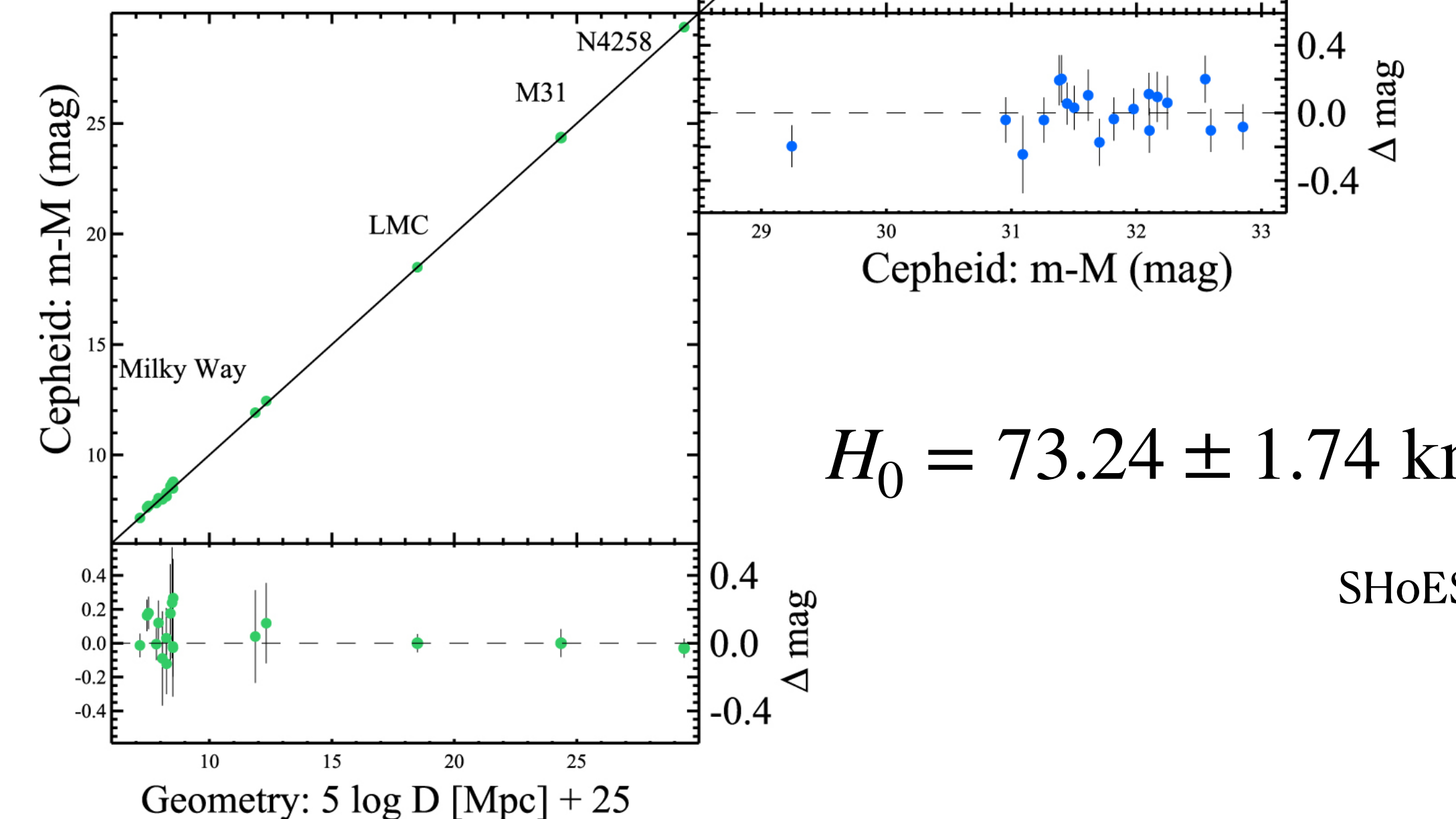
- Geometry to Cepheids
  - Cepheids to Type Ia SN

(Riess et al 2016)

## Cepheids → Type Ia Supernovae

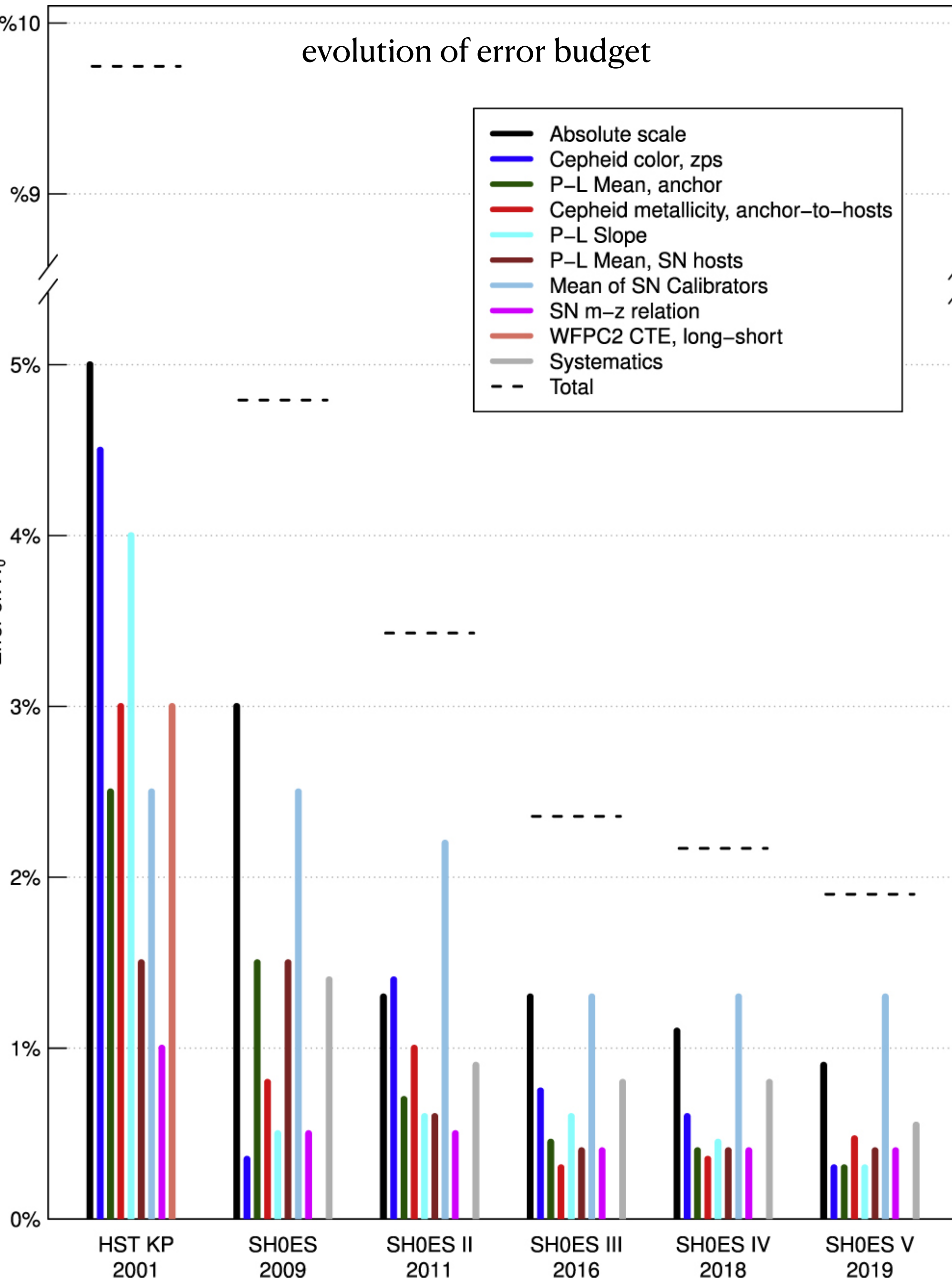


## Geometry → Cepheids



$$H_0 = 73.24 \pm 1.74 \text{ km s}^{-1} \text{ Mpc}^{-1}$$

# SHoES (Riess et al 2016)



## Hubble constant tension

Traditional distance ladder measurements favor  $H_0$  in the low-to-mid 70s.

These are “local,” low redshift measurements (“late” in red at right).

Multi-parameter fits to power spectrum data from the CMB and large scale structure favor  $H_0$  in the mid-to-upper 60s. The CMB is from higher redshift (“early” in blue at right).

The difference is formally significant at over  $4\sigma$ . This becomes  $17\sigma$  if we take the recent Tully-Fisher uncertainty at face value!

**The tension appears to be real**

